

Original Article

Cite this article: Bröcker M (2023) The jadeitites from Syros and Tinos, Cycladic Blueschist Unit, Greece: field observations, mineralogical, geochemical and geochronological characteristics. *Geological Magazine* **160**: 1586–1606. <https://doi.org/10.1017/S0016756823000602>

Received: 12 May 2023

Revised: 23 August 2023

Accepted: 14 September 2023

First published online: 16 October 2023

Keywords:

jadeitite; replacement-type; precipitation-type; U–Pb geochronology; zircon xenocrysts; mélange

Corresponding author:

Email: michael.broecker@uni-muenster.de

The jadeitites from Syros and Tinos, Cycladic Blueschist Unit, Greece: field observations, mineralogical, geochemical and geochronological characteristics

Michael Bröcker 

Institut für Mineralogie, Universität Münster, Münster, Germany

Abstract

This study illustrates the field relationships of jadeitite-bearing block-in-matrix sequences on Syros and Tinos, Cycladic Blueschist Unit, and adds additional U–Pb zircon ages for jadeitites to the geochronological database. The results confirm the importance of Cretaceous (*c.* 80 Ma) and Eocene (*c.* 50 Ma) processes in their geological evolution. Interpretations suggesting that the jadeitites were formed by complete metasomatic replacement of a pre-existing rock are not fully supported by field observations. In at least some cases, the formation of jadeitite is likely due to precipitation from Na–Al–Si-rich aqueous fluids, which also caused variable metasomatic alteration of the host rock. Unambiguous age constraints for formation of the Syros and Tinos jadeitites are not available. A relationship to Eocene blueschist facies metamorphism recorded in the associated metamafic rocks seems plausible. However, since high-pressure overprinting of pre-Eocene jadeitite is also conceivable, there is a much larger time window for jadeitite formation, framed by Cretaceous (*c.* 80–76 Ma) protolith ages of various mélange blocks and the waning stages of blueschist facies metamorphism (*c.* 40 Ma). Field observations are consistent with the interpretation that the mélange-like occurrences on Syros and Tinos record, to varying extent, multi-stage processes that include detachment of mafic rocks from the subducting plate, local infiltration of Na–Al–Si-rich aqueous fluids, exhumation via a serpentinitic matrix in a subduction channel and reworking of the primary block-in-matrix fabric by sedimentary or tectonic processes during accretionary wedge formation.

1. Introduction

Jadeitite *sensu stricto* is a relatively rare rock type that mainly consists of near-endmember jadeite-rich clinopyroxene (>90 vol% pyroxene with on average at least 80 mol% jadeite; Harlow *et al.* 2015). Such rocks occur as isolated bodies within serpentinite or in serpentinitic mélanges together with high-pressure/low-temperature (HP/LT) metamorphic rocks (e.g. Harlow & Sorensen, 2005; Yui *et al.* 2010; Tsujimori & Harlow, 2012; Harlow *et al.* 2015, and references therein). Most jadeitites are interpreted to have formed at $P < 2.0$ GPa and $T < 500$ °C (e.g. Harlow *et al.* 2015), but temperatures >550 °C were also reported for some occurrences (e.g. García-Casco *et al.* 2009; Schertl *et al.* 2012; Angiboust *et al.* 2020, 2021). Petrogenesis of jadeitites is often controversial and associated either with strong metasomatism and replacement of felsic protoliths (R-type) or with precipitation (P-type) from aqueous fluids in veins, or a combination of both processes (e.g. Harlow & Sorensen, 2005; Tsujimori & Harlow, 2012; Harlow *et al.* 2015, and references therein). In either case, jadeitite formation requires circulation of Na–Al–Si-rich fluids. The fluids for the formation of P-type jadeitites originate from the dehydration of a descending slab in a subduction zone or from crystallization of trondhjemitic melts (e.g. Harlow *et al.* 2015; Cárdenas-Párraga *et al.* 2012, 2021). In the case of R-type jadeitites, the most plausible precursors are felsic igneous rocks (e.g. Coleman, 1961; Mori *et al.* 2011; Compagnoni *et al.* 2012; Hertwig *et al.* 2016, 2021; Angiboust *et al.* 2020, 2021). Understanding the mode of formation is of importance for the evaluation of U–Pb zircon data since the assessment of their geological relevance depends crucially on the petrogenesis of the host rocks (e.g. Fu *et al.* 2010, 2012). Furthermore, as jadeitite formation is not restricted to the eclogite and blueschist facies, these rocks may have a different metamorphic age than spatially associated HP/LT rocks (Tsujimori & Harlow, 2012; Harlow *et al.* 2015), adding further complexities to the interpretation of their geological history.

The focus of this paper is on jadeitites from the Cycladic Blueschist Unit (CBU) of Syros and Tinos and describes their field relations, mineralogy, geochemistry and U–Pb zircon geochronology. Although the importance of Cretaceous ages for the heterogeneous block populations of both islands is well documented (e.g. Keay, 1998; Bröcker & Enders, 1999;

© The Author(s), 2023. Published by Cambridge University Press. This is an Open Access article, distributed under the terms of the Creative Commons Attribution licence (<http://creativecommons.org/licenses/by/4.0/>), which permits unrestricted re-use, distribution and reproduction, provided the original article is properly cited.



Tomaschek *et al.* 2003; Bröcker & Keasling, 2006; Bulle *et al.* 2010), uncertainties remain as to when the jadeitites were formed in relation to high-pressure metamorphism and by which process. A particular concern of this study is to improve the geochronological database, which is currently limited to U–Pb zircon ages for only one sample from each of the two islands (Bröcker & Enders, 1999; Bröcker & Keasling, 2006), which may not cover the entire time span of jadeite formation. Furthermore, the question arises whether there are significant differences in the origin of the jadeite and metamafic block-bearing sequences on Syros and Tinos.

2. Regional geology

The Attico-Cycladic Crystalline Belt (ACCB) represents a major tectonostratigraphic unit of the Hellenides and is mainly exposed in the central Aegean region (Fig. 1a). The ACCB comprises two major tectonic units with different P–T–D–t histories, both consisting of numerous fault-bounded subunits (e.g. Dürr *et al.* 1978; Dürr, 1986; Forster & Lister, 2005; Ring *et al.* 2010). The Upper Cycladic Unit includes a heterogeneous sequence of unmetamorphosed Permian to Miocene sediments, Jurassic and undated ophiolitic and metamorphic sole remnants, greenschist-facies rocks with Cretaceous to Palaeogene metamorphic ages as well as Late Cretaceous amphibolite-facies rocks and granitoids (e.g. Altherr *et al.* 1994; Patzak *et al.* 1994; Sanchez-Gomez *et al.* 2002; Kuhlemann *et al.* 2004; Be'eri-Shlevin *et al.* 2009; Martha *et al.* 2016; Lamont *et al.* 2020a). Evidence for HP/LT metamorphism, which is a key feature in the metamorphic history of the structurally lower sequences, was not reported. The upper units were juxtaposed by low-angle detachments onto the nappe stack of the CBU (e.g. Avigad & Garfunkel, 1989; Brichau *et al.* 2007; Jolivet & Brun, 2010; Jolivet *et al.* 2010).

The CBU consists of several tectonic subunits representing a meta-ophiolitic mélange and a metamorphosed volcano-sedimentary passive margin succession (e.g. Dürr 1986; Okrusch & Bröcker 1990; Forster & Lister, 2005; Ring *et al.* 2010; Glodny & Ring, 2022; and references therein), which can be assigned to an upper and lower group of nappes (Grasemann *et al.* 2018; Glodny & Ring, 2022). The lower group was affected by peak conditions of 400 ± 20 °C and 1.0 ± 0.2 GPa, whereas the upper group records temperatures and pressures of 550 ± 50 °C and 2.0 ± 0.2 GPa (Grasemann *et al.* 2018). Numerous geochronological studies documented a polyphase Eocene to Miocene metamorphic history, which includes an eclogite- to epidote blueschist-facies event (c. 55–40 Ma) and later overprinting at lower pressure blueschist-, greenschist- or amphibolite-facies P–T conditions (e.g. Altherr *et al.* 1979; Okrusch & Bröcker, 1990; Wijbrans *et al.* 1990; Bröcker *et al.* 1993; Tomaschek *et al.* 2003; Lagos *et al.* 2007; Ring *et al.* 2010; Bröcker *et al.* 2013; Laurent *et al.* 2016, 2017, 2021; Cliff *et al.* 2017; Peillod *et al.* 2017; Lamont *et al.* 2020b; Glodny & Ring, 2022).

Greenschist-facies rocks at structurally deep levels of Tinos, Evia, Samos, separated from the structurally higher sequences by thrust faults, and regional amphibolite-facies metamorphic rocks at deep levels on Naxos do not record earlier HP/LT conditions or only lower grade blueschist metamorphism than the CBU and are interpreted to be para-allochthonous units (Avigad & Garfunkel, 1989; Ring *et al.* 1999; Shaked *et al.* 2000; Lamont *et al.* 2019). In the case of Tinos, this has not yet been clearly confirmed (Bröcker & Franz, 2005).

In the southern Cyclades (e.g. Ios, Sikinos), the CBU is underlain by gneisses and schists of a pre-Alpine crystalline basement (e.g. van der Maar, 1980; van der Maar & Jansen, 1983), which was also affected by HP/LT metamorphism (Perraki & Mposkos, 2001; Wolfe *et al.* 2023). Detrital zircon geochronology implies a continuous stratigraphic record and provenance evolution and thus a para-autochthonous relationship between basement and the CBU (Flansburg *et al.* 2019; Poulaki *et al.* 2019). Between c. 17 and 11 Ma, the Cyclades were intruded by numerous I- and S-type granitoids (e.g. Altherr *et al.* 1982; Bolhar *et al.* 2010).

3. Local geology

On Syros Island (Fig. 1b), two lithostratigraphic subunits occur structurally above the CBU: the Vari gneisses and a greenschist-facies mylonite sequence (e.g. Ridley, 1984; Trotet *et al.* 2001a, 2001b; Keiter *et al.* 2011; Soukis & Stockli, 2013). These rocks were either not affected by HP/LT metamorphism or do not preserve such mineral assemblages and most likely represent down-faulted tectonic slices representing the hanging wall of the subduction zone complex (e.g. Ridley, 1984; Soukis & Stockli, 2013). The Vari subunit mainly consists of quartzofeldspathic orthogneisses with early Triassic (c. 244–240 Ma) protolith ages of the granitic precursor (e.g. Keay, 1998; Keiter *et al.* 2011; Soukis & Stockli, 2013). Geochemical characteristics indicate an affinity to volcanic arc granites (M. Engel, unpub. Ph.D. thesis, Johannes Gutenberg-Universität, Mainz, 2006). White mica geochronology (^{40}Ar – ^{39}Ar and Rb–Sr) and zircon overgrowths (U–Pb) provided two groups of Late Cretaceous ages (c. 100–95 Ma and c. 75 Ma), interpreted to constrain the time of upper greenschist- to epidote amphibolite-facies metamorphism (Maluski *et al.* 1987; Tomaschek *et al.* 2000). The tectonic contact with the CBU, considered to be a low-angle normal fault (Ridley, 1984), is roughly delineated by a thin sequence of greenschist-facies mylonitic schists, phyllites and minor serpentinite, interpreted as a distinct subunit at the base of the orthogneisses (Bröcker & Enders, 2001; Keiter *et al.* 2011; Soukis & Stockli, 2013). This detachment was active at c. 9–12 Ma, as evidenced by zircon fission-track data (Ring *et al.* 2003).

The structurally lower sequences mostly represent the CBU (e.g. Dixon & Ridley, 1987; Keiter *et al.* 2011) and include several lithostratigraphic or tectonic subunits, which are separated by ductile shear zones (Laurent *et al.* 2016; Kotowski *et al.* 2022; Uunk *et al.* 2022).

A particularly striking feature is an HP/LT mélange, which is best exposed in northern Syros (Kamos mélange; Fig. 1b; e.g. Dixon & Ridley, 1987), but most parts of Syros consist of marble-schist sequences. The significantly greater thickness of the marbles compared to the neighbouring islands of Tinos and Andros probably results from tectonic repetition by thrusting or isoclinal folding (e.g. Dixon & Ridley, 1987; Keiter *et al.* 2011).

The Syros nappe stack was affected by HP/LT metamorphic conditions up to c. 1.3–2.2 GPa and 450–550 °C, but at different times, and variable degrees of lower pressure overprinting (e.g. Trotet *et al.* 2001a, 2001b; Keiter *et al.* 2004; Schumacher *et al.* 2008; Philippon *et al.* 2011; Laurent *et al.* 2017; Uunk *et al.* 2018, 2022; Skelton *et al.* 2019; Ring *et al.* 2020; Gorce *et al.* 2021; Kotowski *et al.* 2022; Glodny & Ring, 2022).

Various geochronologic methods (^{40}Ar – ^{39}Ar , K–Ar, Rb–Sr, U–Pb, Sm–Nd, Lu–Hf) documented the importance of Eocene HP/LT metamorphism (55–40 Ma) for both the Kamos mélange and other CBU subunits (e.g. Maluski *et al.* 1987; Bröcker & Enders, 2001; Tomaschek *et al.* 2003; Putlitz *et al.* 2005; Lagos *et al.* 2007;

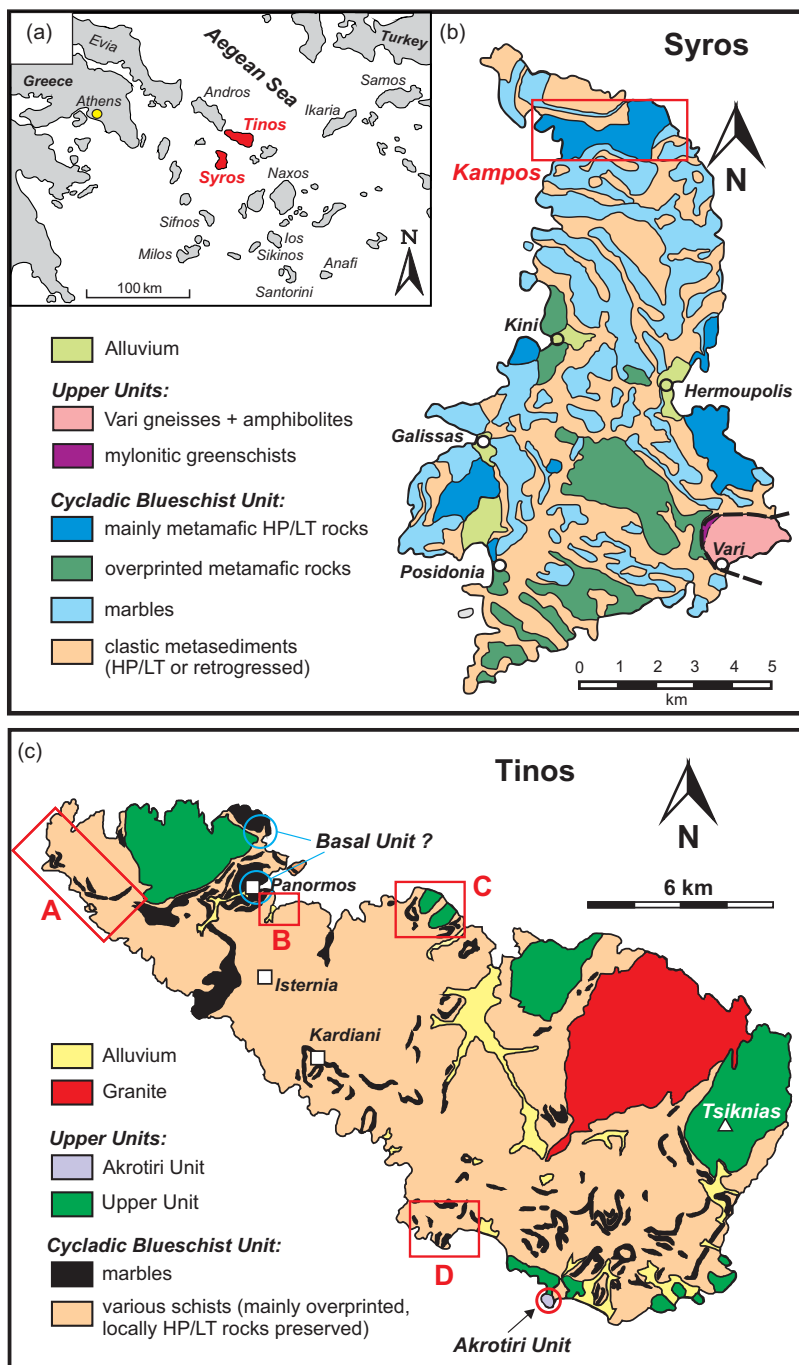


Figure 1. (Colour online) (a) Geographic overview of the larger study area. (b, c) Simplified geological maps of Syros (modified after Keiter *et al.* 2004) and Tinos (modified after Melidonis, 1980). Red rectangle in (b) outlines Kampos area. Red rectangles in (c) show areas where blocks occur more frequently in the schist sequences. A = NW Tinos; B = Panormos; C = Mavra Gremna; D = Kionia.

Bröcker *et al.* 2013; Cliff *et al.* 2017; Skelton *et al.* 2019; Gorce *et al.* 2021; Kotowski *et al.* 2022; Uunk *et al.* 2022, 2018; Tual *et al.* 2022). The geological relevance of younger white mica dates has been attributed either to incomplete resetting or to distinct exhumation increments (e.g. Bröcker *et al.* 2013; Rogowitz *et al.* 2015; Cliff *et al.* 2017; Laurent *et al.* 2017; Uunk *et al.* 2018; Glodny & Ring, 2022). The marble-schist sequence records only minor, localized evidence for Miocene ages (~ 21 Ma) that are common elsewhere in the Cyclades (e.g. Bröcker *et al.* 2013; Kotowski *et al.* 2022). Tomaschek *et al.* (2008) also described a tectonic slice of the Cycladic basement within the basal part of the CBU.

On Tinos Island (Fig. 1c), the metamorphic succession can be subdivided into at least three tectonic subunits, referred to in the

local literature as the Akrotiri Unit, the Upper Unit, and the Lower Unit (e.g. Melidonis, 1980; Okrusch & Bröcker, 1990; Katzir *et al.* 1996). The Akrotiri and Upper subunits (Fig. 1c), which form the uppermost part of the metamorphic sequence, belong to the regional Upper Cycladic Unit and record amphibolite and greenschist-facies P–T conditions (e.g. Patzak *et al.* 1994; Katzir *et al.* 1996; Bröcker & Franz, 1998; Zeffren *et al.* 2005; Lamont *et al.* 2020a). Field observations as well as lithological and metamorphic similarities indicate a correlative relationship with the two upper subunits on Syros (Bröcker & Enders, 2001; Soukis & Stockli 2013).

The Akrotiri Unit (300–350 m thick) comprises a relatively small occurrence near the main town of the island (Fig. 1c) and mainly consists of an interlayered amphibolite-gneiss sequence

(Patzak *et al.* 1994). *P*–*T* estimates indicate metamorphic pressures of 0.6–0.85 GPa and temperatures of *c.* 490–610 °C (Patzak *et al.* 1994). *K*–*Ar* hornblende and white mica dating of amphibolites and gneisses yielded apparent ages of *c.* 77–66 Ma and *c.* 60–53 Ma, respectively (Patzak *et al.* 1994). The contact to other subunits is not exposed, but judging from general field relationships this gneiss-amphibolite sequence forms the uppermost part of the Tinos metamorphic succession. The position of the Akrotiri rocks within the overall structural architecture of the region is not yet fully understood. The Akrotiri rocks either belong to a specific tectonic subunit on top of the CBU, e.g. the Asteroussia nappe, or are related to the local Tsiknias metamorphic sole (Patzak *et al.* 1994; Katzir *et al.* 1996; Lamont *et al.* 2020a).

The Upper Unit (at least 750 m thick) includes serpentinites, meta-gabbros, meta-plagiogranites, amphibolites, ophicalcites and listvenites that are embedded in, or are structurally underlain, by mostly mafic phyllites (Melidonis 1980; Katzir *et al.* 1996; Bröcker & Franz, 1998; Zeffren *et al.* 2005; Hinsken *et al.* 2017; Lamont *et al.* 2020a; Mavrogonatos *et al.* 2021). The metamorphic history of the various rock types includes upper greenschist to amphibolite-facies ocean floor metamorphism, greenschist-facies overprinting during Oligocene–Miocene orogenic processes and formation of a metamorphic sole that is locally partially melted (Katzir *et al.* 1996; Bröcker & Franz, 1998; Zeffren *et al.* 2005; Lamont *et al.* 2020a). Jurassic U–Pb zircon protolith ages for a plagiogranitic sill (*c.* 162 Ma) and a meta-gabbro (*c.* 144 Ma) imply a correlative relationship of the Tsiknias occurrence (Fig. 1c) to the Pelagonian ophiolites of the Greek mainland (Lamont *et al.* 2020a). Zircons of leucodioritic melt pockets in the sole amphibolites yielded a zircon overgrowth U–Pb age of 74.0 ± 3.5 Ma (Lamont *et al.* 2020a), which overlaps with the *K*–*Ar* dates of the Akrotiri amphibolites. *K*–*Ar*, ^{40}Ar – ^{39}Ar and *Rb*–*Sr* dates of other Upper Unit rocks (mafic and pelitic phyllites, meta-gabbros) range from 95 to 13 Ma and were related to variable age resetting during juxtaposition-related ductile deformation (Bröcker & Franz, 1998; Zeffren *et al.* 2005). The Upper Unit was placed on top of the Lower Unit by a low-angle normal fault (e.g. Avigad & Garfunkel, 1989; Katzir *et al.* 1996; Brichau *et al.* 2007) during a regional greenschist-facies episode at *c.* 21 Ma, which also affected the underlying CBU (Bröcker & Franz, 1998).

The Lower Unit (*c.* 1250–1800 m in thickness), recently interpreted as consisting of several subunits with different tectonic and thermal histories (Lamont *et al.* 2020b), belongs to the regional CBU and comprises mainly siliciclastic metasediments, marbles as well as mafic and felsic meta-volcanic rocks (e.g. Melidonis, 1980; Bröcker *et al.* 1993; Hinsken *et al.* 2016; Lamont *et al.* 2020b). Hinsken *et al.* (2016) reported Late Cretaceous (*c.* 80–70 Ma) maximum depositional ages (MDAs) for the lithostratigraphic succession above the lowermost dolomite marble, which contains Triassic fossils (Melidonis, 1980). Remnants of HP/LT rocks or mineral assemblages are common, but pervasively retrogressed greenschist-facies rocks are more widespread (e.g. Melidonis, 1980; Bröcker *et al.* 1993; Breeding *et al.* 2003; Bulle *et al.* 2010; Lamont *et al.* 2020b).

Metamorphic conditions of the HP/LT event originally were estimated at ~1.2–2.0 GPa and 450–550 °C (e.g. Bröcker *et al.* 1993; Parra *et al.* 2002). More recent petrological modelling suggests peak *P*–*T* conditions of ~2.0–2.6 GPa and 490–570 °C (Lamont *et al.* 2020b). The highest *P*–*T* conditions were reported for blueschists and eclogites from the Kionia area, which represents the topmost part of the Lower Unit (Lamont *et al.* 2020b). For rocks from deeper structural levels, Lamont *et al.* (2020b)

described *P*–*T* conditions of ~1.85 GPa and 480–510 °C for the HP stage and of ~0.7 GPa and 500–540 °C for the retrograde greenschist overprint. According to Parra *et al.* (2002), overprinting during exhumation includes decompression from 1.5–1.8 GPa at 500 °C to 0.9 GPa at 400 °C, a thermal overprint (400–550 °C, ~0.9 GPa) and further decompression from 0.9 GPa at 550–570 °C to 0.2 GPa at 420 °C. White mica dating indicated Eocene white mica ages for HP/LT rocks (*c.* 44–40 Ma) and ages between 36 and 21 Ma for greenschist-facies rocks (e.g. Bröcker *et al.* 1993, 2004; Bröcker & Franz, 1998). More recently, Glodny and Ring (2022) argued that blueschist-facies conditions lasted from at least *c.* 36 to 33 Ma and reported a *c.* 22 Ma age for the greenschist-facies overprint. Bulle *et al.* (2010) and Hinsken *et al.* (2016) described U–Pb zircon rim data of *c.* 57–46 Ma and related these ages to the HP/LT stage.

The lowermost part of the metamorphic sequence is exposed in NW Tinos near Panormos (Fig. 1c) and consists of greenschist-facies dolomite marbles and minor sedimentary phyllites, which have been interpreted either as a para-autochthonous Basal Unit (Avigad & Garfunkel, 1989) or as an integral part of the Lower Unit (Melidonis, 1980; Bröcker & Franz, 2005). In eastern Tinos (Fig. 1c), the emplacement of Miocene I- and S-type granitoids (*c.* 15–14 Ma; Altherr *et al.* 1982; Bröcker & Franz, 1998; Keay, 1998; Brichau *et al.* 2007) has caused contact metamorphism in both the Upper Unit and the Lower Unit (Avigad & Garfunkel, 1989; Bröcker & Franz, 1994, 2000; Stolz *et al.* 1997).

4. Field description

4.a. The Kamos mélangé on Syros

The Kamos mélangé is shown on geological maps as a distinct lithological or tectonic subunit (e.g. Dixon & Ridley, 1987; Keiter *et al.* 2004, 2011), but at least the inferred upper tectonic contact is not well established. The mélangé includes blocks and tectonic slices (<1 m to several hundred metres) of various eclogite- and blueschist-facies rocks such as meta-gabbros, eclogites, glaucophanites, ultrabasic rocks, jadeitites and interlayered bimodal metavolcanic rocks, which are partly exposed by erosion from a matrix of altered ultramafic rocks or clastic metasediments (Fig. 2; e.g. Dixon & Ridley, 1987; Seck *et al.* 1996; Bröcker & Enders, 2001; Breeding *et al.* 2004; Keiter *et al.* 2004, 2011; Marschall *et al.* 2006; Ague 2007; Miller *et al.* 2009; Bulle *et al.* 2010; Gyomlai *et al.* 2021). Many blocks are still in contact with sheared serpentinite or chlorite- and talc-rich schists derived from an ultramafic precursor (Fig. 2b, e). Prominent blackwall alteration zones are widespread due to metasomatic interaction with serpentinitic host rocks (e.g. Dixon & Ridley, 1987; Bröcker & Enders, 2001; Miller *et al.* 2009; Gyomlai *et al.* 2021). *P*–*T* estimates for blackwall formation range from ~1.2 GPa and 500–550 °C (Breeding *et al.* 2004) to 0.6–0.7 GPa and 400–430 °C (Marschall *et al.* 2006) or 1.2 GPa and 430 °C (Miller *et al.* 2009). Discrete serpentinite blocks are locally preserved. Whole rock major and trace element geochemistry and stable isotope data (δD and $\delta^{18}\text{O}$) of serpentinites suggest an origin in an extensional tectonic setting, such as a hyper-extended margin or a mid-ocean ridge and fracture zone environment (Cooperdock *et al.* 2018).

Siliciclastic metasediments also occur as host rocks for mafic and felsic blocks (Fig. 2c–f; Dixon & Ridley, 1987; Keiter *et al.* 2011), particularly in the upper part of the mélangé zone. Metamorphosed mafic blocks in a matrix of blueschists and quartz mica schists have also been reported from rock sequences below

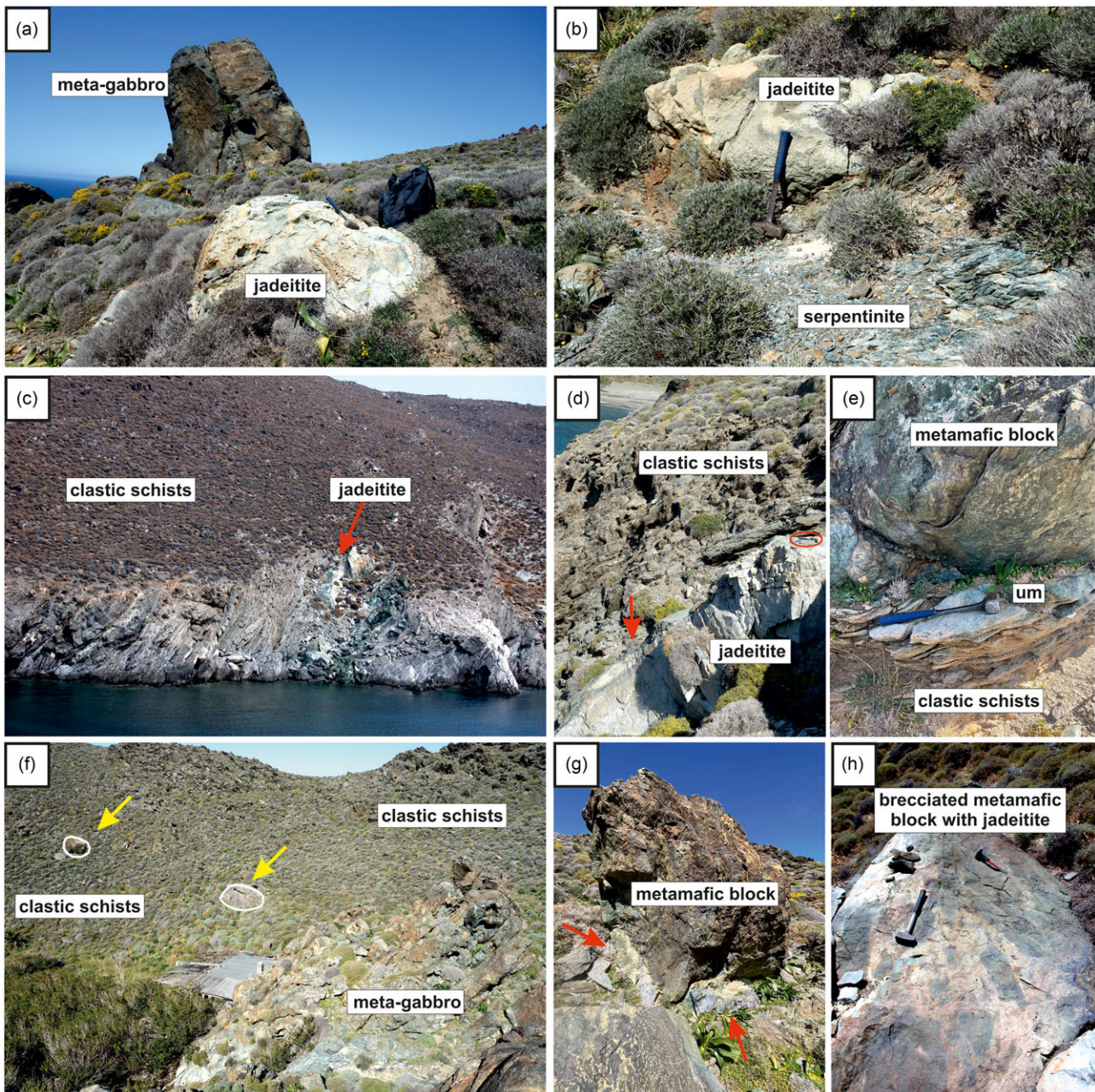


Figure 2. (Colour online) Field images from the Kampos mélangé, Syros. (a) Jadeitite and meta-gabbro blocks (GPS: N 37° 29.582; E 24° 54.301). (b) Jadeitite-serpentinite contact (GPS: N 37° 29.603; E 24° 54.663). (c, d) Jadeitite in mainly clastic metasedimentary host rocks (GPS: N 37° 29.581; E 024° 54.037). (e) Metamafic block with thin selvage of altered ultramafic schists (=um, with hammer on it) within clastic metasediments (GPS: N 37° 29.569; E 24° 54.093). (f) Blocks of variably sized glaucophane-rich rocks (yellow arrows) and meta-gabbro in clastic metasedimentary schists. (g) Close-up of the leftmost block in the previous image (GPS: N 37° 29.688; E 24° 53.955). Red arrows point to blackwall zones. (h) Lower half of the brecciated eclogite-jadeitite block (GPS: N 37° 29.603; E 24° 54.558). Hammer for scale, marked by red ellipse in (d), is 40 cm in length.

the Kampos mélangé and its correlative equivalents (Laurent *et al.* 2016; Kotowski & Behr, 2019), but the focus here is on jadeitite-bearing occurrences. For detailed field descriptions of the Kampos mélangé see Dixon and Ridley (1987) and Gyomlai *et al.* (2021).

The Kampos block population includes rock fragments with Cretaceous (*c.* 80–75 Ma) U–Pb zircon ages (e.g. Keay, 1998; Tomaschek *et al.* 2003; Bröcker & Keasling, 2006; Supplementary Table S1) attributed to either igneous crystallization or to metamorphic or hydrothermal processes. Some tectonic fragments yielded a Triassic (*c.* 245–240 Ma) protolith age (Bröcker & Keasling, 2006). Such ages were also reported for similar rocks

from structurally lower CBU sequences (Tomaschek *et al.* 2003), suggesting that tectonic slices originating from disruption of a primary lithostratigraphic unit were also incorporated in the mélangé. However, most of the blocks are interpreted as remnants of oceanic lithosphere from a back-arc basin (Seck *et al.* 1996; Keay, 1998).

The modal and geochemical variability of the metamafic rocks has been linked to the development of their protoliths in different magma chambers (Seck *et al.* 1996). Protoliths of the coarse-grained metamafic rocks were interpreted to represent gabbros affected to varying degrees by fractional crystallization, while the

precursors of finer-grained metamorphosed mafic rocks were associated with ocean floor basalts (e.g. Dixon & Ridley, 1987; Seck *et al.* 1996). Protolith ages of matrix rocks are poorly constrained. Clastic metasedimentary rocks from the Kampos area indicate a Late Cretaceous MDA (c. 95–70 Ma; Keay, 1998; Löwen *et al.* 2015).

Explanations for the origin of the block-in-matrix sequences on Syros include mechanical mixing by olistostromatic or tectonic processes (e.g. Dixon & Ridley, 1987; Bröcker & Enders, 2001; Bulle *et al.* 2010) and concepts based on the exposure of mafic and ultramafic rocks on the seafloor in a hyper-extended intra-oceanic setting combined with rheological heterogeneities of subducted rock types (e.g. Kotowski & Behr, 2019, 2022; Gyomlai *et al.* 2021).

4.b. The Tinos block-in-matrix sequence

Occurrences of metamorphosed mafic blocks in a metasedimentary matrix were recognized in NW-Tinos, near Kionia, SE of Panormos and in the Mavra Gremna area (labelled A, B, C and D in Fig. 1c). However, unlike northern Syros, there is not a clearly defined and mappable *mélange* subunit. Instead, from the top to the base of the Lower Unit, relatively few isolated blocks of meta-gabbros, glaucophanites, eclogites, jadeitites and ultramafic rocks (mostly <1–10 m, but up to 300 m) occur at various levels within the marble-schist sequence (Bröcker & Enders, 1999; Bulle *et al.* 2010). The block-forming process is controversial. Bulle *et al.* (2010) assumed a meta-olistostromatic origin. In contrast, Lamont *et al.* (2020a) attributed the blocks to boudinage of mafic lithologies. The block population records HP/LT metamorphic conditions and includes rock types like those in the Kampos *mélange* (Figs. 3, 4a–c), but their abundance is much smaller, and the matrix consists almost entirely of metasedimentary or meta-tuffaceous rocks. Especially noteworthy is the existence of jadeitites (Figs. 3a, b; 4a–c). Ultramafic rocks are rare (e.g. Lamont *et al.* 2020b), but some metamafic blocks are surrounded by a thin serpentinite or chlorite schist cover (Bulle *et al.* 2010), suggesting that these blocks were originally in contact with an ultramafic matrix. Ion probe dating of eclogite, glaucophanite, blackwall and chlorite schist yielded Cretaceous U–Pb zircon ages (c. 80 Ma; Bulle *et al.* 2010; Supplementary Table S1). Similar MDAs have been reported from the enclosing schists, implying that detritus derived from the block-forming mafic lithologies also occurs in the metasediments (Bulle *et al.* 2010; Hinsken *et al.* 2016). In various parts of the Lower Unit, meta-conglomerate horizons are associated with the block-in-matrix succession (Fig. 4d–e; Bulle *et al.* 2010).

5. Analytical methods

Mineral compositions were determined with a JEOL 8530F electron microprobe (EMP). Natural and synthetic mineral standards were used for calibration. Operating conditions were a 15 kV accelerating voltage, 5 nA electron beam current and a 5- μ m spot size. Counting times were 5 s on the peak and 2 s on the background.

For U–Pb geochronology, zircon crystals were separated from several kilograms of fresh rock by standard routines (jaw crusher, disc mill, Wilfley table, Frantz magnetic separator, methylene iodide heavy liquid and handpicking under stereomicroscope). After preparation of epoxy resin mounts and polishing to expose grain interiors, cathodoluminescence (CL) imaging was applied to reveal the internal zircon structures and to guide spot placement.

Ion microprobe (SHRIMP) dating was carried out at the Centre of Isotopic Research (VSEGEI), St. Petersburg, Russia. Analytical procedures followed standard operating routines and were similar to those reported by Bulle *et al.* (2010) and Bröcker *et al.* (2014). Individual spot ages in Supplementary Table S5 are based on the ^{207}Pb correction method, assuming $^{206}\text{Pb}/^{238}\text{U}$ – $^{207}\text{Pb}/^{235}\text{U}$ age-concordance. Most analyses contain very little common Pb and thus are insensitive to the choice of initial isotopic composition. Weighted averages (without error in standard) and intercept ages are quoted as $^{206}\text{Pb}/^{238}\text{U}$ ages with 95% confidence limit and 2σ uncertainty, respectively. The uncorrected data for all samples are presented in Tera–Wasserburg diagrams. Such plots, regressions and weighted mean age calculations are based on Isoplot 4.15 (Ludwig, 2012).

Bulk-rock compositions were analysed by Actlabs, Ancaster, Ontario, applying a lithium metaborate/tetraborate fusion technique followed by acid digestion and analysis by ICP and ICP/MS (4Lithoresearch analytical protocol).

6. Petrography and mineralogy

Nineteen samples were selected for more detailed petrographic, geochemical and geochronological investigation. Samples from Syros are from the Kampos area (Fig. 1b). Samples from Tinos were collected in various parts of the island (Fig. 1c). GPS coordinates of sampling locations are reported in Supplementary Table S2 (available online at <https://doi.org/10.1017/S0016756823000602>). Field images are shown in Figs. 2–4. Hand specimen images are presented in Fig. 5. Photomicrographs are depicted in Figs. 6 and 7. EMP analyses with the focus on clinopyroxene compositions are summarized in Supplementary Table S3.

Many of the samples examined are not jadeite *sensu stricto* but variably albitized or impure jadeitites with lower jadeite contents. Fresh or poorly overprinted jadeitites are massive, non-foliated and granoblastic rocks with mostly light-green colour (Fig. 5). With increasing degree of retrograde overprinting, the colour changes to darker shades of green. Apart from possibly zircon, no igneous relicts or pseudomorphs of such phases were found.

The primary mineral assemblages mainly consist of jadeite and variable modal amounts of white mica, epidote, amphibole, zircon and titanite (Figs. 6, 7). Some samples also contain quartz (e.g. sample 4030). Pristine clinopyroxene is high in jadeite component (Jd > 80 mol.%; Fig. 8; Supplementary Table S3) and occasionally shows oscillatory zoning. The most abundant retrograde phase is albite (Figs. 6a–f; 7d) with nearly end-member composition (Supplementary Table S3). Retrograde overprinting is also indicated by omphacitic rim compositions of clinopyroxene and small grains or overgrowths of aegirine-augite (Figs. 6f; 8a, b). In general, jadeitites from Syros are better preserved than similar rocks from Tinos.

On Tinos, two petrographic and geochemical types of jadeite-rich rocks can be distinguished: The first type (sample 4011) corresponds to similar rocks from Syros and occurs as loose block in association with various schists and marble (Figs. 3a, b; 4a–c). More strongly overprinted derivatives of such rocks are exposed in the Panormos area both as in-situ block within meta-tuffaceous schists (samples 5535, 5537, 5539; Fig. 4a, b) and as loose boulders (sample 9028; Fig. 4c). Despite severe retrogression, unoriented and mostly fine-grained jadeite (up to Jd > 90 mol.%) is still preserved (Fig. 8e; Supplementary Table S3). The second type (sample 1049) is restricted to a small occurrence near Kionia (Fig. 1c) and was originally described as jadeite (Bröcker &

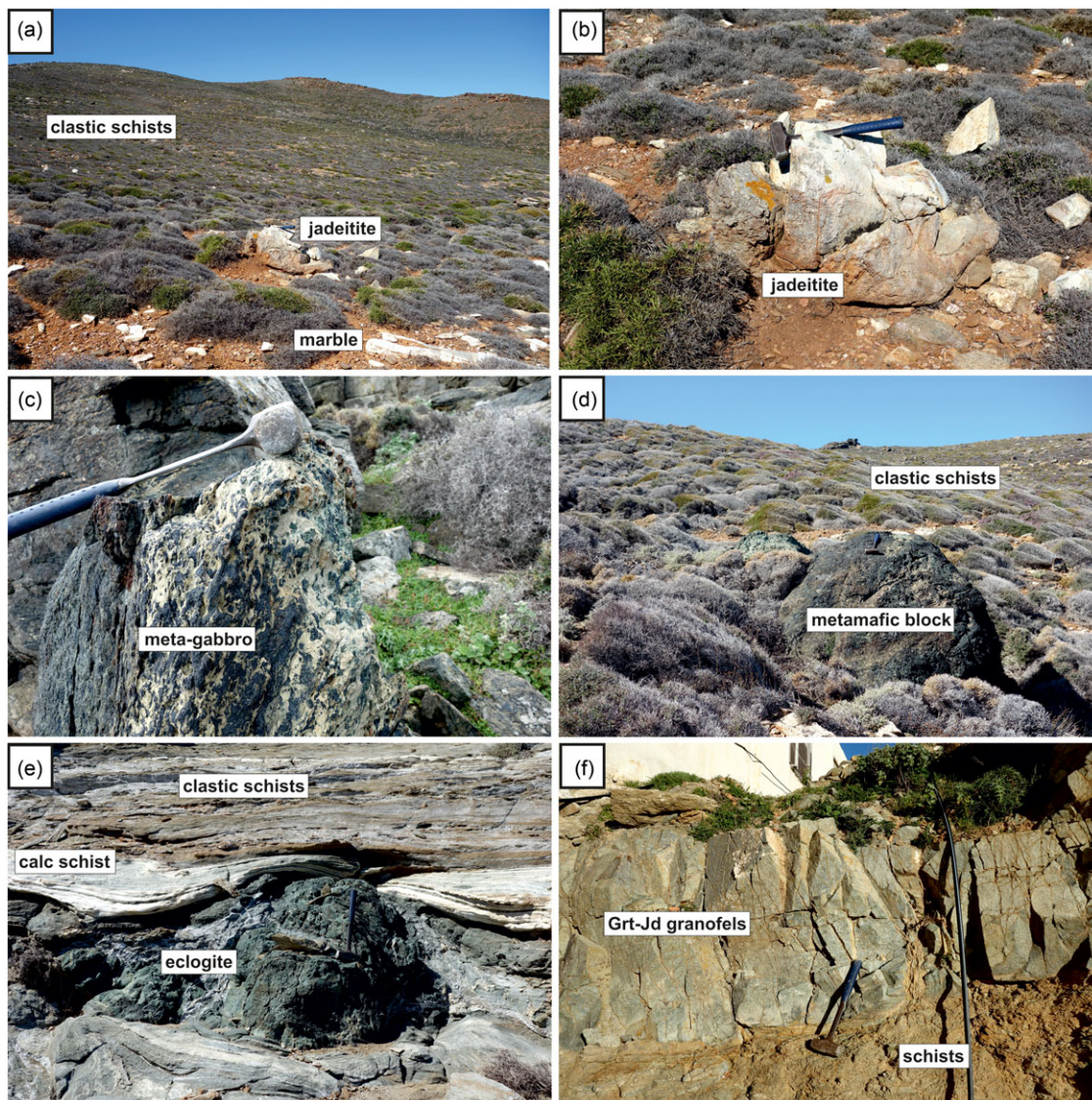


Figure 3. (Colour online) Field images from the Mavra Gremna and Kionia areas, Tinos. (a) Isolated jadeitite block (sample 4011) in marble-schist sequence. (b) Close-up of jadeitite block 4011 (GPS: N 37° 38.809; E 025° 07.180). (c) HP/LT metamorphic meta-gabbro (GPS: N 37° 38.809; E 25° 07.224). (d) Metamafic block in clastic schists (GPS: N 37° 38.867; E 25° 07.358). (e) Boudinaged eclogite block in metasedimentary host rocks (GPS: N 37° 39.040; E 25° 07.184). (f) Kionia garnet-jadeite granofels (GPS: N 37° 33.483; E 25° 07.767). Hammer for scale is 40 cm in length.

Enders, 1999) but is more aptly defined as garnet-jadeite granofels, as the mineral composition often contains significant amounts of garnet (Fig. 7g, h). Many hand samples are very similar to eclogite, but the clinopyroxenes are jadeites (Fig. 8f). Most of the original outcrop was destroyed by the construction of a house, but a small part remained and shows the garnet-jadeite granofels in metasedimentary schists (Fig. 3f).

Samples 5171, 5175 and 5176 represent the mafic parts of the compound eclogite-jadeitite block (Fig. 2h; stop 11 in the excursion guide of Dixon & Ridley, 1987; for additional outcrop pictures see Bröcker & Keasling, 2006). The mineral assemblage of the newly dated sample 5175 (Fig. 6g) is dominated by sodium-rich clinopyroxene (>70 vol.%) and relatively little garnet (5–10 vol.%). Epidote, white mica and rutile occur as additional primary phases. Glaucofane, titanite and chlorite are related to a later overprint. Sample 5171 was collected from a different part of the net-veined block and has less garnet than the other two samples but

shows cross-cutting omphacitic clinopyroxene veins (Fig. 6 h, i). The compositions of matrix and vein clinopyroxenes partially overlap, but the veins include abundant crystals with lower Jd component (Fig. 8c; Supplementary Table S3).

7. Whole rock geochemistry

Analytical results are summarized in Supplementary Table S4. On a volatile-free basis, normalized to 100%, the jadeitites from Syros have intermediate to high SiO₂ (57.8–76.3 wt.%), moderate to high Al₂O₃ (13.6–19.6 wt.%) and Na₂O (5.7–11.9 wt.%) as well as variable MgO (0.6–4.6 wt.%), total Fe₂O₃ (1.1–5.1 wt.%) and CaO (0.2–6.5 wt.%) concentrations. MnO, K₂O and P₂O₅ contents are mostly very low (<0.1 wt.%, <0.2% and <0.1 wt.%, respectively). TiO₂ is in the range from 0.2 to 1.1 wt.%. Jadeitites from Tinos (samples 4011 and 5539) are characterized by intermediate SiO₂ (57.6–58.1 wt.%) combined with high Al₂O₃ (20.0–21.3 wt.%) and

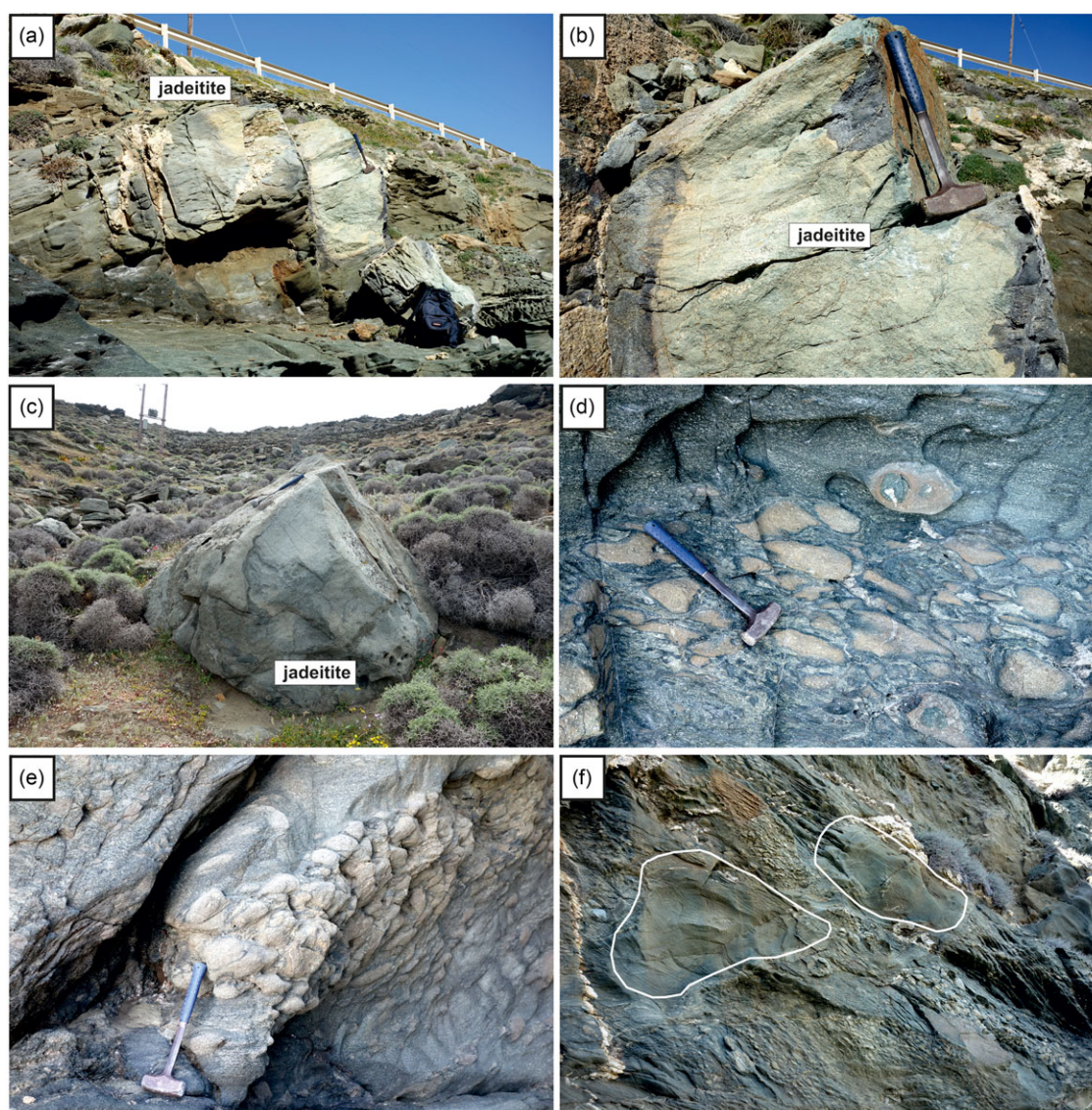


Figure 4. (Colour online) Field images from the Panormos area, Tinos. (a) In-situ jadeitite block in green meta-tuffaceous schists in the coastal cliff north of Rochari beach (samples 5535, 5537, 5539; GPS: N 37° 38.982; E 25° 03.475). (b) Close-up of block shown in previous image with haematite-rich alteration along the block margin. (c) Strongly retrogressed jadeitite block from the coastal cliff area north of Rochari beach (samples 9028, 9029; GPS: N 37° 38.875; E 25° 03.740). (d, e) Monomict volcaniclastic meta-conglomerates (GPS: N 37° 38.893; E 25° 03.709 and N 37° 38.885; E 25° 03.697). (f) Olistoliths in meta-conglomeratic matrix (GPS: N 37° 38.885; E 25° 03.697). Hammer for scale in (a–e) is 40 cm in length. Field of view in (f) about 6 m wide.

high Na₂O (10.0–10.5 wt.%). Samples 4011 and 5539 are similar in composition to the Syros jadeitites, except the high K₂O concentration (2.1 wt.%) of sample 5539, while the Kionia garnet-jadeite samples (1045, 1049, 1050) have significantly higher total Fe₂O₃ (8.9–10.0 wt.%). MgO (2.0–2.3 wt.%) and CaO (3.6–3.8 wt.%) are in the range of the Syros samples. MnO (<0.25 wt.%), K₂O (<0.3%) and P₂O₅ (<0.1 wt.%) are very low. Harker diagrams show decreasing values of TiO₂, Al₂O₃, FeO, MnO, CaO and Na₂O with increasing SiO₂ (Fig. 9). Among the trace elements, the high Zr concentrations (up to 2000 ppm) of the Kionia samples are particularly noticeable.

There are no significant bulk-rock compositional differences between jadeitites from Syros and Tinos (Figs. 9, 10). In MORB-normalized multi-element diagrams, the jadeitites and the garnet-jadeite rocks show similar distribution patterns with enrichment in high HFSE and negative troughs for at K, Sr and Ti and flat REE

trends (Fig. 10a, c, e). However, based on normalized REE patterns, different groups can be distinguished. The first group is characterized by distribution patterns with distinct negative Eu anomalies (Eu/Eu* = 0.38–0.71; Fig. 10b). Samples of the second group show almost horizontal sinusoidal REE variations (Fig. 10d). Three jadeitites of the third group show enrichments of the LILE and a negative REE slope (Fig. 10f). The REE pattern of sample 5260 differs from all other samples by having a positive Eu anomaly (Eu/Eu* = 1.9; Fig. 10c).

8. U–Pb geochronology

CL images of zircon are shown in Fig. 11 and U–Pb analytical data are reported in Fig. 12 and Supplementary Table S5. For all dated samples, zircon O–Hf isotope data were already reported by Fu *et al.* (2010, 2012).

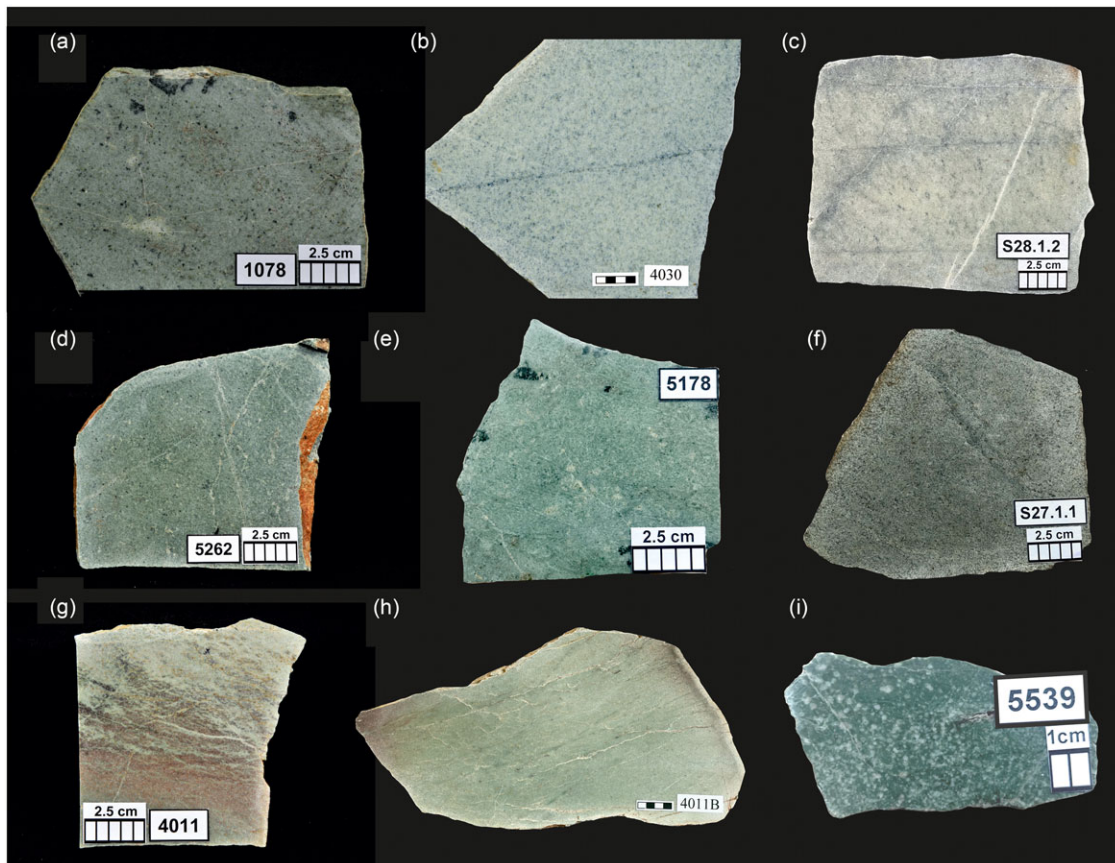


Figure 5. (Colour online) Hand specimen pictures of jadeitites from Syros and Tinos.

In all samples, zircon typically has a short prismatic or blocky morphology. Pristine grains or domains show mostly rhythmic zoning or sector-zoned internal patterns, but many crystals have complex cauliflower-like internal structures, indicating partial recrystallization (Fig. 11). Inherited cores or distinct overgrowths were not observed, but some zircon grains of sample 1049 have dark, irregularly shaped, recrystallized domains.

Sample 1078 (Figs. 5a; 6a, b) was collected from a loose block in the upper part of the path to Lia beach, just after the gate. The quartz-bearing jadeitite 4030 (Figs. 5b; 6c, d) represents the block shown in Fig. 2c, d (stop 15 in the excursion guide of Dixon & Ridley, 1987). Ion probe dating of samples 1078 and 4030 yielded almost identical anchored intercept ages of 80.7 ± 1.7 Ma and 81.7 ± 1.3 Ma, respectively (Fig. 12a, b).

Sample 3148 represents the jadeitite from the eclogite-jadeitite net-veined rock with distinct blackwall alteration zones (stop 11 of Dixon & Ridley, 1987). This sample was dated in a previous study (Bröcker & Keasling, 2006) and is presented here with new data evaluation. The screened data give an intercept age of 79.8 ± 0.4 Ma (Fig. 12c), which only slightly differs in the uncertainty from the original age calculation. From this outcrop, the mafic host rock, represented by sample 5175 (Fig. 6g), was also dated. Eight zircon spot analyses provided an intercept age of 78.0 ± 1.0 Ma (Fig. 12d).

Sample 4011 (Figs. 5g, h; 7a–c) was collected in the Mavra Gremna area on Tinos where it occurs as loose boulder together with widely scattered metamorphosed mafic blocks within a marble-schist sequence (Fig. 3a, b). Ten U–Pb spot analyses yielded an intercept age of 82.6 ± 1.6 Ma (Fig. 12e). Sample 1049 (garnet-jadeite granofels) from Kionia was included in this study

to check the geological significance of a previously reported TIMS multigrain zircon date (Bröcker & Enders, 1999). U–Pb zircon data define a lower intercept age (not anchored) of 75.0 ± 3.1 Ma and a geologically meaningless upper intercept (Fig. 12f). A recrystallized domain gave the youngest spot age of 52.2 ± 2.1 Ma (spot 10.1; Fig. 11f). The weighted mean $^{206}\text{Pb}/^{238}\text{U}$ age is 78.6 ± 1.9 Ma (spot 10.1 excluded). For all other samples, the weighted average ages are nearly identical to the intercept ages (Supplementary Table S5).

9. Discussion

9.a. Zircon geochronology and bulk-rock compositions

One aim of this study was to expand the small geochronological dataset for jadeitites from the Cyclades and to resolve ambiguities of existing multigrain TIMS zircon data. In the case of Syros, it was easy to select additional samples as virtually all jadeitites of the Kampos area are zircon-rich. The situation is more difficult on Tinos, where jadeitites are much rarer and only occasionally contain zircon.

The newly dated samples from both islands yielded U–Pb intercept ages of *c.* 83–80 Ma and almost identical weighted average $^{206}\text{Pb}/^{238}\text{U}$ ages (Fig. 12a–c, e; Supplementary Table S5). The metamafic host rock and cross-cutting jadeitite of a brecciated eclogite-jadeitite block yielded U–Pb ages of 78.0 ± 1.0 Ma and 79.8 ± 0.4 Ma, respectively, which overlap within analytical uncertainty (Fig. 12c, d; see also Bröcker & Keasling, 2006). Taken together, these data document that there is only a single age group of jadeitites on Syros and Tinos.

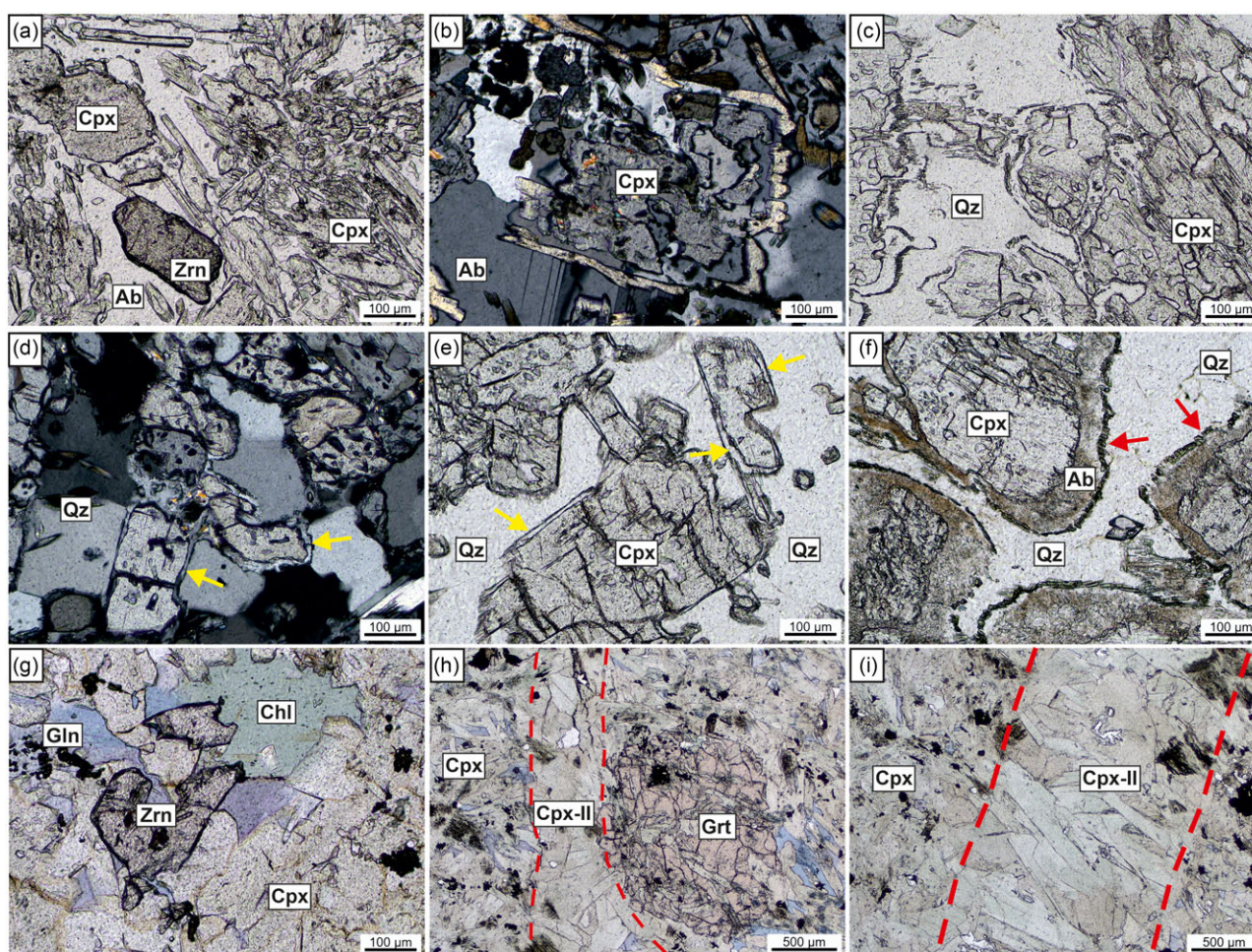


Figure 6. (Colour online) Thin section images of samples from the Kampos area, Syros. (a, b) Jadeite 1078. (c, d) Jadeite 4030. (e) Jadeite S28.1. (f) Jadeite S27.1. (g) Eclogite 5175. (h, i) Eclogite 5171. Yellow arrows in (d, e) point to retrograde albite around jadeite. Red arrows in (f) indicate newly formed aegirine augite. Red dashed lines in (h, i) roughly delineate younger veins. Ab, albite; Chl, chlorite; Cpx, clinopyroxene; Gln, glaucophane; Qz, quartz; Zrn, zircon.

Based on normalized REE patterns, different groups of jadeitites and jadeite-rich rocks can be distinguished (Fig. 10b, d, f). This variability in composition may be related to derivation from different plagiogranitic protoliths, such as described from the Oman and Troodos ophiolites (e.g. Rollinson, 2009; Freund *et al.* 2014), to metasomatic alteration of a single protolith type by fluids of variable composition, to direct precipitation from different jadeite-forming fluids, to differences in modal abundance of accessory phases or to changes in REE signatures during retrograde processes. At this stage, this aspect cannot be further clarified because, among others things, no geochemical data are available for potential felsic protoliths. A special case is the in-situ occurrence of garnet-jadeite granofels near Kionia (Figs. 1c, 3f). This rock has a very Zr-rich rock bulk-rock composition (c. 1700–2000 ppm) and corresponding zircon abundance (Fig. 7g, h), which is also typical for a very small occurrence of loose eclogite fragments (Zr: c. 3500–5000 ppm) located a few hundred metres away at the foot of the same hill (Bröcker & Enders, 1999, 2001).

The bulk-rock composition of the garnet-jadeite samples can be clearly distinguished from the Tinos jadeitites (samples 4011 and 5539), but their REE patterns are very similar to those of Syros samples 3148 and 1077 (Fig. 10). Oscillatory-zoned jadeite (Fig. 7i) and the similarity of trace element and rare earth distribution patterns to those of a sample representing fracture-filling jadeite

indicate original crystallization in an open system and a P-type formation mode. However, in contrast to the Kampos mélangé, which locally hosts jadeitites in metasedimentary schists (Fig. 2c), there is no evidence here of subsequent tectonic or sedimentary incorporation of foreign material into the host rock, such as remnants of a serpentinized matrix or blackwall alteration around the granofels as a result of initial contact with ultramafic matrix. Thus, this outcrop could represent a boudin of an extrusive or intrusive meta-igneous layer or vein, as postulated by Lamont *et al.* (2020b) for the formation of metamafic blocks in the Tinos schist sequences. However, it should be emphasized that there is no general evidence for a boudinage origin of the block-in-matrix occurrences on Tinos. Isolated metamafic blocks (meta-gabbro, eclogite, glaucophanite) and jadeitites occur sporadically in schists. There are no lithological horizons of such rocks that are continuously or discontinuously exposed over longer distances. In addition, blackwall alteration and altered ultramafic schists around blocks have also occasionally been described from the Tinos metamafic blocks (Bulle *et al.* 2010), suggesting incorporation of exotic material by tectonic or sedimentary reworking. In any case, the Kionia garnet-jadeite rocks and eclogites are unusual and rare lithologies that are not known anywhere else in the CBU.

In a previous study, multigrain U–Pb zircon TIMS dates of c. 63–61 Ma were reported for sample 1049 from the Kionia in-situ

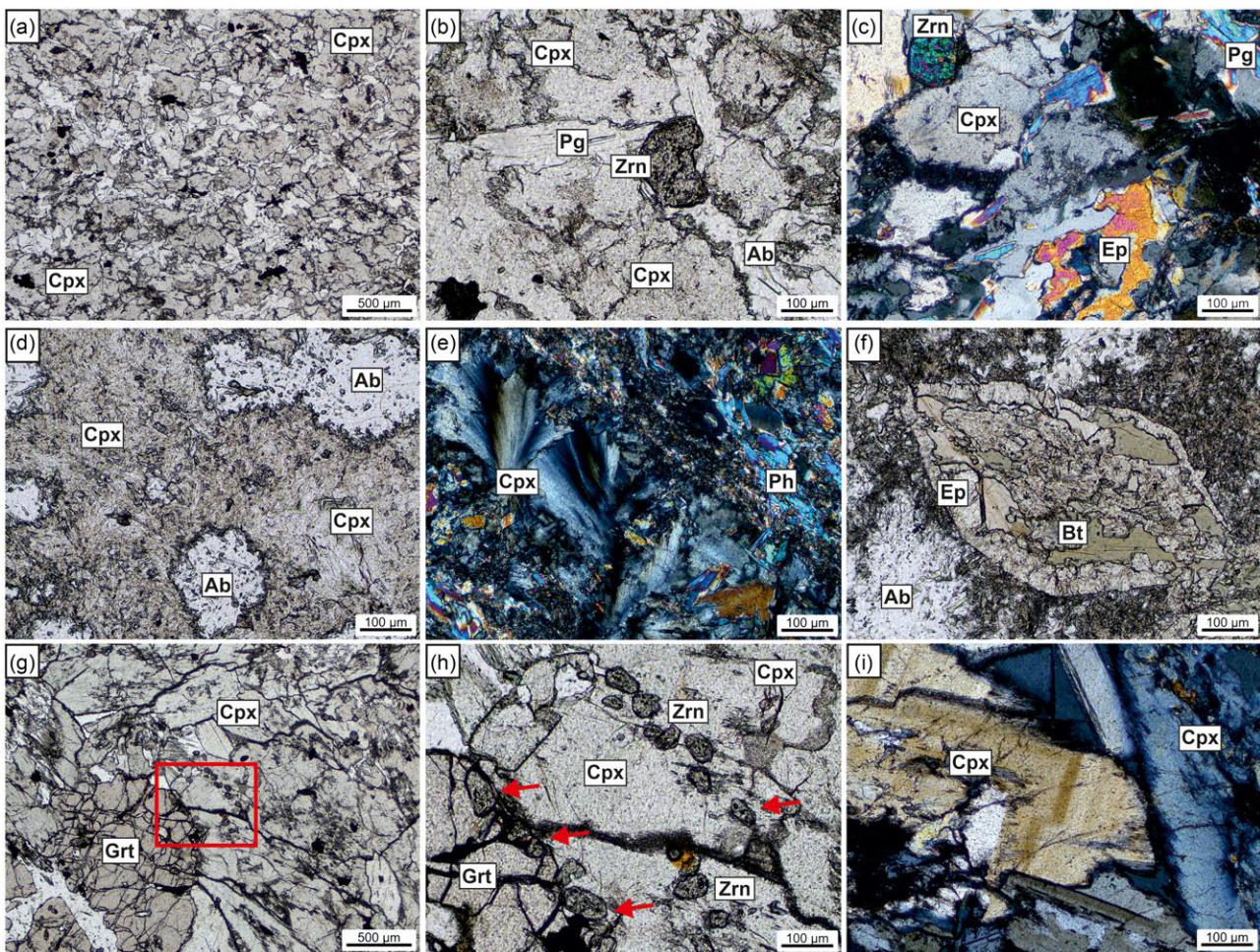


Figure 7. (Colour online) Thin section images of samples from various locations on Tinos jadeitites and garnet-jadeite granofels from Tinos. (a, b, c) Jadeitite 4011, Mavra Gremna area. (d) Overprinted jadeitite 5535. (e, f) Strongly overprinted jadeitite 9028, Panormos area. (g, h, i) Garnet-jadeite granofels 1049, Kionia area. Red rectangle in (g) outlines area shown as close-up in (h). Red arrows in (h) point to zircon grains in and around garnet: Ab, albite; Bt, biotite; Chl, chlorite; Cpx, clinopyroxene; Ep, epidote; Grt, garnet; Pg, paragonite; Ph, phengite; Zrn, zircon.

outcrop (Bröcker & Enders, 1999). This apparent age is not confirmed by ion probe dating of zircons from the same sample, which instead yielded a U–Pb intercept age of 75 ± 3.1 Ma and a single spot age of *c.* 50 Ma for a recrystallized domain (Fig. 11; Supplementary Table S5). Similar Cretaceous (78.2 ± 1.4 Ma) and Eocene (*ca.* 57–54 Ma) U–Pb ages were reported for a Kionia eclogite (Bulle *et al.* 2010).

9.b. Relationship between zircon and jadeite formation

In the central Aegean region, jadeitites occur on the islands of Syros, Tinos and Andros (Fig. 1a). In terms of bulk-rock composition, the age complexity of the zircon population and the protolith age, the jadeitite from Andros differs significantly from similar rocks on the neighbouring islands (Höhn *et al.* 2022). Particularly striking is the more complex zircon population of the only dated sample, which is characterized by Jurassic overgrowths (163.1 ± 3.9 Ma and 174.3 ± 2.0 Ma) on Middle Proterozoic (*c.* 1126 Ma and *c.* 1421 Ma) and Permian (*c.* 273 Ma and *c.* 281 Ma) grains (Bulle *et al.* 2010), indicating an R-type origin. It is very likely that the Andros occurrence belongs to another tectonic subunit within the nappe stack of the CBU (Höhn *et al.* 2022).

The jadeitites from Syros and Tinos are different. These rocks yielded Late Cretaceous U–Pb zircon ages (*c.* 80 Ma; Fig. 12; Supplementary Table S5), as did the zircons from spatially associated metamafic mélangé rocks, which are interpreted as protolith ages. Similar observations in the Rio San Juan Complex, Dominican Republic, led to the conclusion that the jadeitite protoliths were part of the oceanic crust before subduction (Hertwig *et al.* 2021). However, since the samples studied here are from a mélangé, it is possible that rocks of the same age, formed in different ways and in different places, were mixed later in the subduction channel or during tectonic or sedimentary reworking.

The significance of zircon in jadeitites (inherited or newly formed?) is often controversial, and the different interpretations proposed for the jadeitites of Syros and Tinos are a good example of such controversies. Early studies interpreted the U–Pb ages of jadeitites and related blackwall zones as indication for Cretaceous metamorphic or hydrothermal subduction zone processes (Bröcker & Enders, 1999; Bröcker & Keasling, 2006). This explanation was challenged in later studies, which instead argued for an igneous zircon origin, based on mantle-like oxygen isotope ratios and initial epsilon hafnium values of zircons (Fu *et al.* 2010, 2012), similar interpreted protolith ages of associated eclogites and

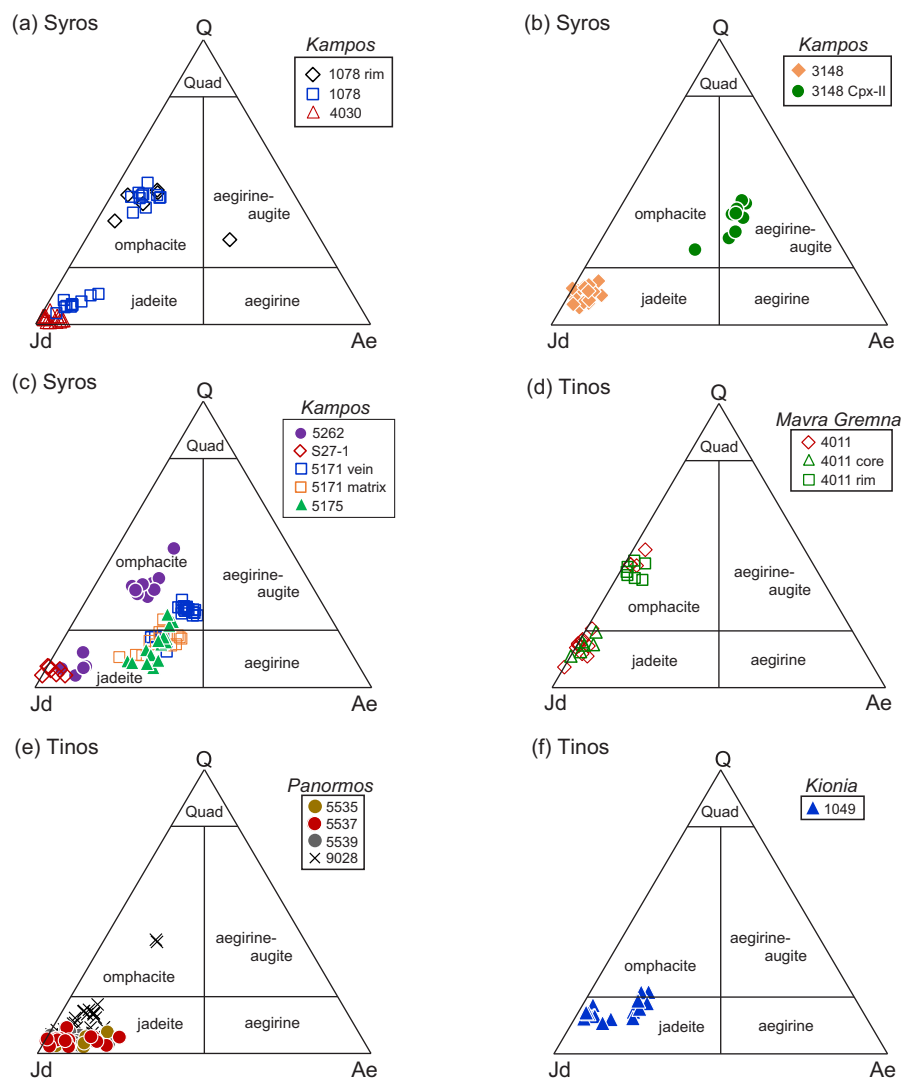


Figure 8. (Colour online) Compositions of clinopyroxenes in the classification diagram of Morimoto *et al.* (1988).

meta-gabbros and a re-evaluation of presumed high-pressure mineral inclusions as pseudo-inclusions (Tomaschek *et al.* 2003; Fu *et al.* 2010). These arguments led to the conclusion that the jadeitites were formed by complete metasomatic replacement of a pre-existing meta-igneous rock during Eocene HP/LT metamorphism recorded in other CBU rocks (Fu *et al.* 2010, 2012). However, the petrogenesis of the studied jadeitites does not seem to be related to the formation of blackwalls at the contacts between blocks and ultramafic matrix, as some jadeitite blocks, like other lithologies, also show such reaction rinds.

Nevertheless, uncertainties remain regarding the petrogenesis and the timing of jadeitite formation. Eocene HP/LT metamorphism is evident, but the jadeitites may also reveal earlier subduction-related processes under different P–T conditions. There is a much larger time window for jadeitite formation, bracketed by Cretaceous zircon protolith ages (*c.* 80 Ma) of various mélangé blocks, and white mica ages for the waning stages of blueschist facies metamorphism (*c.* 40 Ma).

As discussed below, the conclusion that the jadeitites were formed by metasomatic replacement of a pre-existing rock rather than precipitation from aqueous fluids, with the zircons representing relicts of the igneous protolith (Fu *et al.* 2010, 2012), is not entirely convincing. Most jadeitites are found as

isolated blocks, completely detached from the original site of formation. Only in one case is the original relationship documented by a brecciated eclogite-jadeitite block broken into two larger pieces that show the net-veined block interior very well (Fig. 2h). This structure documents either the forceful injection of felsic melts into already lithified parts of a mafic protolith or the precipitation of jadeitite from vein fluids in fractures. However, this observation does not necessarily mean that the jadeitite formed during the blueschist-facies overprint of pre-existing eclogite (Tsuji-mori & Harlow, 2012). The age of jadeitite formation may be older than both the eclogite- and blueschist-facies P–T stages recorded in other mélangé rocks.

The lack of a resolvable age difference between host rock (78.0 ± 1.0 Ma) and cross-cutting jadeitite (79.8 ± 0.4 Ma; Fig. 12c, d) could be due to the following explanations:

- (a) The igneous origin of both rock types and the intrusive relationship are correctly interpreted. The zircons of both rock types were formed during the same magmatic event before subduction and indicate the protolith age. Both rock types were later metasomatically altered by hydrothermal fluids, with the felsic rock showing pervasive jadeitization, while the mafic host rock was much less affected. Apart

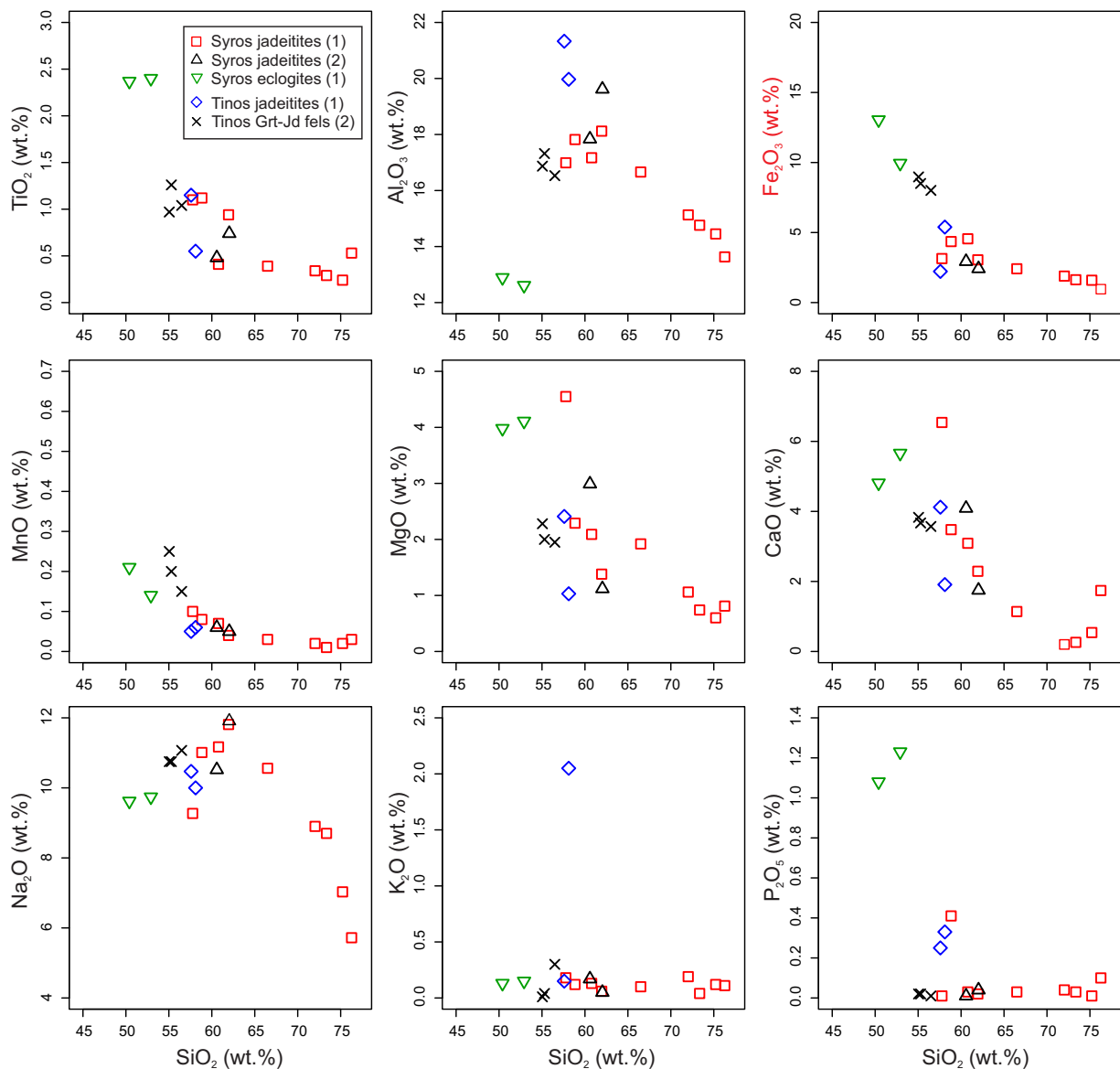


Figure 9. (Colour online) Harker diagrams for jadeitites and eclogites from Syros and Tinos. Data source: (1) = this study; (2) Bröcker and Enders (2001). Diagram was made with GeoChemical Data toolkit (GCDkit, version 6.0; Janoušek *et al.* 2006).

from zircon, no other relics of the original igneous rock are preserved in the jadeitites.

- (b) The parental rocks of the jadeitites are not subducted fragments of the ocean crust but originate from slab-derived melts or from otherwise unrecognized magmatic processes in the Cretaceous subduction zone. The zircons indicate the protolith age. Alternatively, the 80 Ma zircons could represent xenocrysts in subducted or slab-derived magmatic protoliths that do not date the time of partial melting or later jadeitite formation.
- (c) The net-veined block is evidence of hydrothermal or mechanical brecciation of an eclogitic rock and precipitation of jadeitite from Na-Si-Al-rich aqueous fluids. The host rock was also affected to some extent by fluid infiltration. If the igneous origin of the zircons is correct, the zircons in the jadeitite must be fluid-transported xenocrysts that were picked up elsewhere. The time of jadeitite formation

remains undetermined. The 80 Ma zircons of the eclogite give an age of the metamafic protolith.

- (d) The interpretation of a magmatic origin of the zircons is wrong. The existence of contemporaneous zircon in both the host rock and the jadeitite is due to the infiltration of zirconium-rich fluids.

There is currently no fully convincing answer to the question of which of these alternatives apply. The distinction between hydrothermal, igneous or metamorphic zircon is often difficult and ambiguous. Many of the criteria commonly used as distinguishing features, such as Th/U ratios, trace element and REE signatures (e.g. Flores *et al.* 2013), do not provide clear indications of the mode of formation (e.g. Schaltegger, 2007; Bulle *et al.* 2010; Zhong *et al.* 2018). Nevertheless, in the present case, a misinterpretation of the O-Hf zircon characteristics is not very likely. The relatively small compositional range of average $\delta^{18}\text{O}$

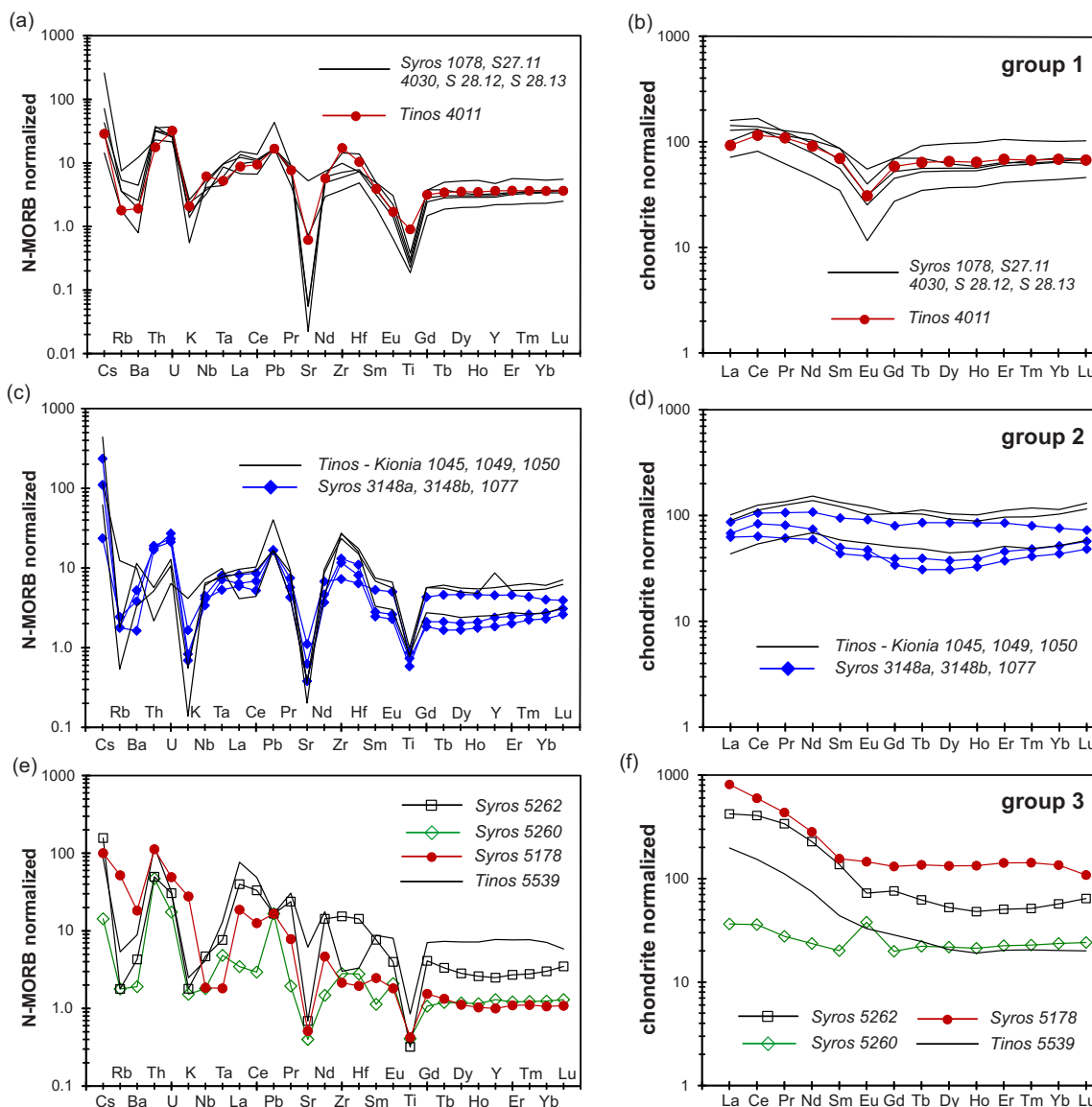


Figure 10. (Colour online) Normalized trace element and REE patterns for jadeitites and eclogites from Syros and Tinos, including data reported by Bröcker and Enders (2001). N-MORB normalization values are from Sun and McDonough (1989). Chondrite normalization values are from McDonough and Sun (1995).

(4.7 % to 5.5 %) and initial $\epsilon_{Hf}(t)$ values (+10 to +24) is consistent with an igneous origin and indicates zircon crystallization from melts that were produced from a depleted mantle source (Fu *et al.* 2010, 2012). However, zircons in jadeitite may be xenocrysts that have been entrained by melt or aqueous fluids. The presence of such zircons in aqueous solutions does not seem to be a particularly realistic hypothesis, but such scenarios have been proposed both for zircon in jadeitites (Meng *et al.* 2016; see also Yui & Fukuyama, 2015) and for zircon in quartz veins cross-cutting eclogite (Sheng *et al.* 2012).

Formation of jadeitite requires hydrothermal fluids that induce metasomatism or direct open-system crystallization in fractures. Field observations indicate that at least some of the studied jadeitites belong to the P-type. Interestingly, oscillatory-zoned clinopyroxenes of some Syros omphacitites suggest a similar origin (see Shigeno *et al.* 2012 for a similar example from western Kyushu, Japan). So far, neither the claim that all jadeitites of Syros are metasomatized rocks nor the age of jadeitite formation has been

conclusively proven. Both aspects require further investigation. Such studies should also take a closer look at the geochemistry of meta-plagiogranitic dykes and melt injections in meta-gabbros as potential precursors of R-type jadeitites, as a direct lineage may be established here. In this context, it is interesting to note that Hertwig *et al.* (2021) reported that jadeite rocks from the Rio San Juan Complex, Dominican Republic, could have been derived from plagiogranites by isochemical replacement or metasomatic desilication without extensive chemical exchange.

9.c. Different origins for the jadeitite-bearing sequences on Syros and Tinos?

A characteristic feature of the Kampos mélangé on Syros is the abundance of blocks within a relatively well-defined and mappable horizon, the presence of both serpentinitic and clastic metasedimentary host rocks and metasomatic reaction rinds at contacts between blocks and ultramafic matrix. On Tinos, only few blocks

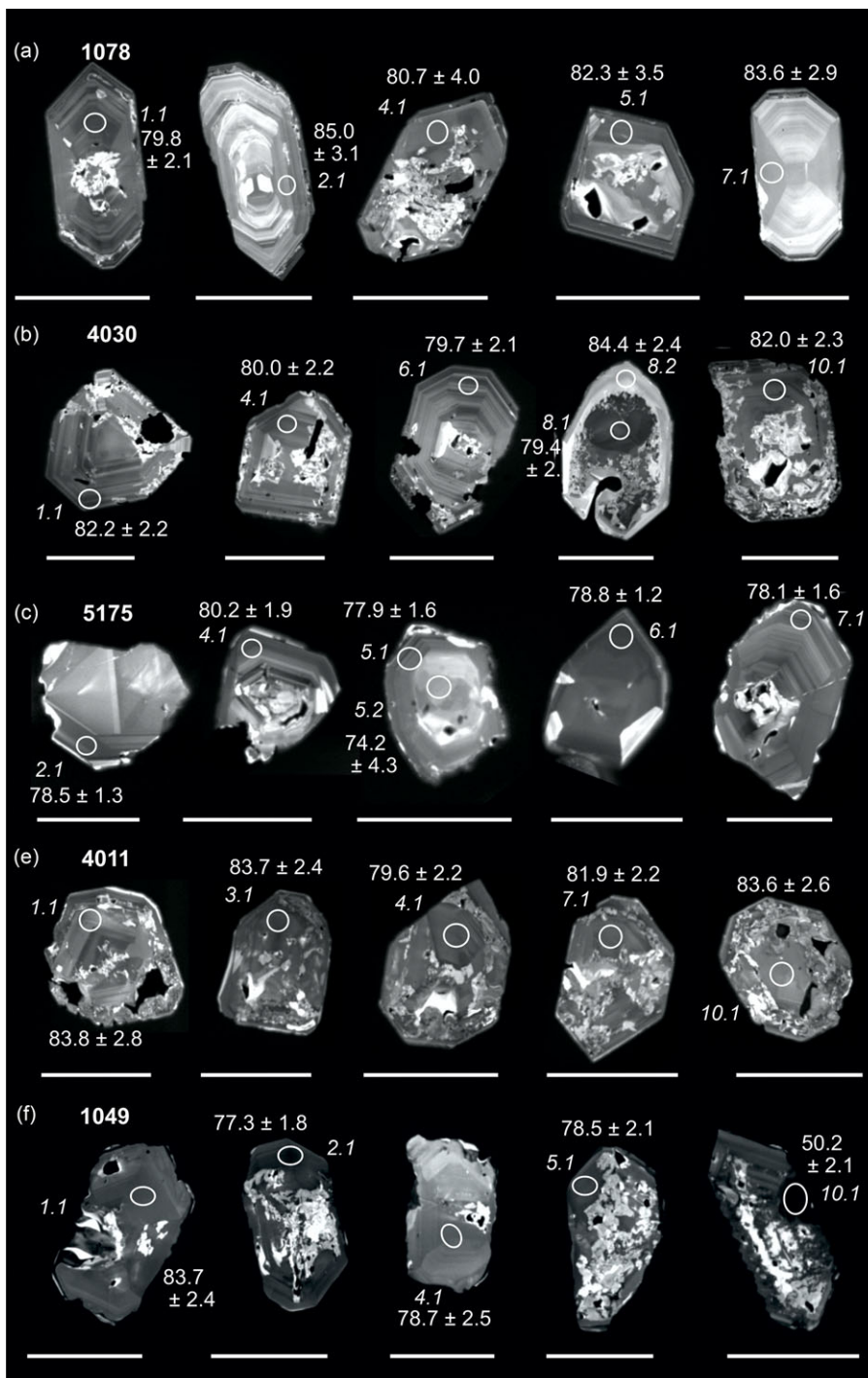


Figure 11. Cathodoluminescence images of representative zircons of U–Pb-dated samples from Syros and Tinos with spot identification numbers and $^{206}\text{Pb}/^{238}\text{U}$ ages (1σ). White lines for scale are 200 μm in length.

occur in metasedimentary and meta-tuffaceous sequences, serpentinite is rare and blackwall rinds around blocks have either never existed or are only sporadically preserved (Bulle *et al.* 2010). In addition, both native and exotic blocks with Triassic and Late Cretaceous U–Pb zircon ages, respectively, have been described from the Kampos mélangé, whereas only exotic Late Cretaceous blocks were reported from Tinos (Keay, 1998; Bröcker & Enders, 1999; Tomaschek *et al.* 2003; Bröcker & Keasling, 2006; Bulle *et al.* 2010). However, upon closer inspection, the differences between the two areas are smaller than first appears. The two block-in-matrix occurrences share many petrographic, geochemical and

geochronological similarities, including that (1) the same rock types occur as blocks (e.g. meta-gabbros, eclogites, glaucophanites, jadeitites, serpentinites), (2) some metamafic mélangé rocks have high Ti or Zr concentrations (e.g. Seck *et al.* 1996; Bröcker & Enders, 2001), (3) mainly Cretaceous U–Pb zircon ages (*c.* 80 Ma) were determined for mélangé blocks, (4) blocks are repeatedly found in metasedimentary host rocks and (5) similar MDAs were reported for block-bearing clastic schists (Bulle *et al.* 2010; Löwen *et al.* 2015; Hinsken *et al.* 2016).

The coincidence of the U–Pb zircon ages of meta-igneous blocks and the MDAs of metasediments led to the interpretation

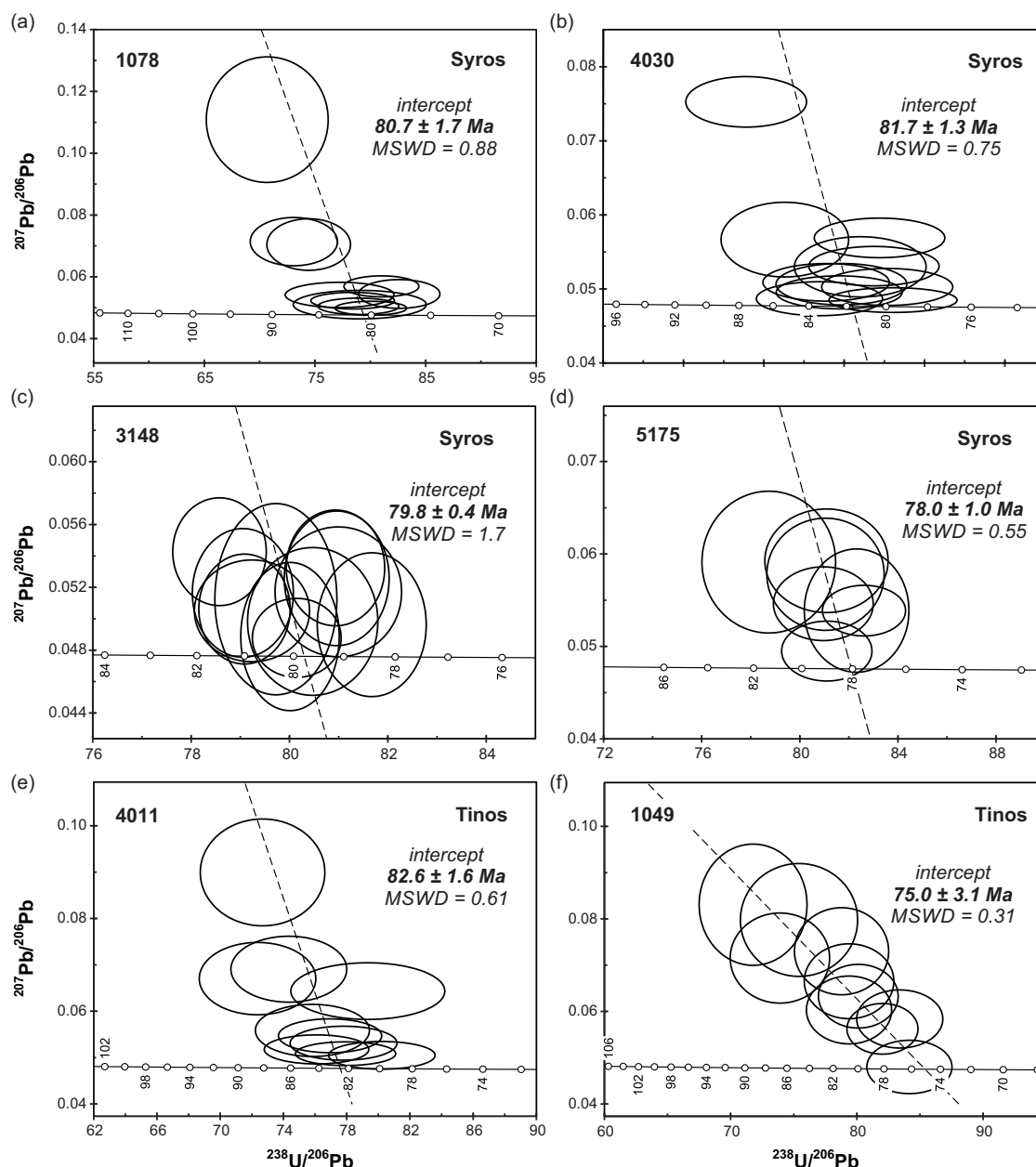


Figure 12. Tera-Wasserburg diagrams of U-Pb-dated samples from Syros and Tinos. Data point error ellipses indicate 1σ uncertainties. Black dashed lines in (a, b, d, e) indicate mixing trend with a common Pb composition anchored at $^{207}\text{Pb}/^{206}\text{Pb}$ values of 0.841 ($t = 78\text{--}83$ Ma; Stacey & Kramers, 1975) and in (c) of 0.9618 (Broken Hill gold). Dashed line in (f) indicates an unanchored mixing trend.

that both blocks and sedimentary detritus of similar age originated from the same source and were mixed during gravity-driven transport (Bulle *et al.* 2010). This explanation was questioned by Lamont *et al.* (2020b) and Kotowski *et al.* (2022). In the case of Tinos, Lamont *et al.* (2020b) argued that the sporadic blocks in a mainly metasedimentary matrix differ significantly from the Kampos mélange on Syros and suggested a primary sedimentary-volcanic origin, with the eclogites representing boudinaged mafic intrusions or lava flows rather than olistoliths. Lamont *et al.* (2020b) compared the field situation on Tinos with the Chroussa subunit on Syros, which also comprises block-bearing coherent sequences (Keiter *et al.* 2011; Laurent *et al.* 2016) and described a lithological difference between the blocks on Tinos, interpreted as

boudins of mafic layers, and the more diverse rock types of the mélange on Syros, interpreted to represent fragments of subducted oceanic crust.

Field observations are not fully consistent with this interpretation. Boudinage at all scales is a common feature on Tinos; however, the same rock types are found in the block population as in the Kampos mélange, including meta-gabbros, eclogites and jadeitites (Figs. 3, 4a–c), but in much smaller numbers. Some of these blocks are surrounded by thin ultramafic or chloritic selvages and blackwall zones (Bulle *et al.* 2010). This suggests that these rocks were originally in contact with a serpentinite matrix before being redeposited into the present host rocks. This is similar to parts of the Kampos area where blocks with a thin ultramafic cover

are found within clastic schists (Fig. 2c, f; e.g. Dixon & Ridley, 1987; Bulle *et al.* 2010; Keiter *et al.* 2011). It is unlikely that such block-in-matrix structures simply record competence contrasts. A non-boudinage-related block-in-matrix fabric for at least parts of the block population is also evident, for example, by the presence of jadeitites. A coarse-grained meta-gabbro lens (up to 300 m in diameter) with preserved magmatic relics (Bulle *et al.* 2010) also supports this interpretation, as sill-like intrusions of such melts are unknown from the Cyclades. In addition, mass flow processes are documented by frequent meta-conglomeratic layers, which locally are associated with larger olistoliths (Fig. 4d–f).

Kotowski *et al.* (2022) pointed out that the ‘mélange’ structure in large parts of Syros does not result from sedimentary or subduction-related tectonic processes but is inherited from the original intra-oceanic setting. These authors concluded that the field relationships can be reconciled by assuming subduction of hyper-extended lithosphere, which led to exposure of mafic and ultramafic rocks on the seafloor by oceanic core complex detachments, followed by subduction along the interface shear zone, return flow in the subduction channel and imbrication (Kotowski *et al.* 2022).

As an argument for rejecting the interpretation of Bulle *et al.* (2010), Kotowski *et al.* (2022) stressed that the presence of apparent young-on-old stratigraphic relationships in the detrital zircon record is not consistent with mechanical mixing during subduction or submarine landslide processes. However, this assessment is not entirely conclusive for several reasons:

(1) The original sequence stratigraphy is not well understood and may involve a more complex internal framework of depositional units and processes than can be resolved by existing detrital zircon data. (2) Detrital zircons do not provide absolute ages but only an upper boundary for the timing of sedimentation. The presumed ‘young-on-old’ structural relationships are therefore not really proven but only inferred. Moreover, such relationships have not been described from Syros but from the Western and Southern Cyclades (Seman *et al.* 2017; Poulaki *et al.* 2019). From northern Syros, Seman (2016) instead reported that two schist samples (Gramatta schists) collected north of the Kampos mélange yielded MDAs (75 ± 5 Ma) that correspond to both the youngest detrital age group of the underlying Kampos schists (Löwen *et al.* 2015) and the interpreted protolith ages of mélange blocks (e.g. Keay, 1998; Tomaschek *et al.* 2003; Bröcker & Keasling, 2006). Seman (2016) proposed a stratigraphic relationship between the two occurrences and considered the Gramatta schists as sedimentary cover of the Kampos sequence.

Taken together, this leads to the conclusion that the recorded sedimentation of northern Syros is consistent with a model suggesting that mass-transport processes played a role in the formation of the block-in-matrix structures. However, the field observations and data can also be reconciled with other interpretations that differ mainly in whether mafic and ultramafic fragments were already exposed on the seafloor before subduction (Kotowski & Behr, 2019; Kotowski *et al.* 2022) or whether fragments of such rocks were later detached from the subducting plate, and in the importance of subsequent tectonic or sedimentary reworking for the incorporation of blocks into their present host rocks (Dixon & Ridley, 1987; Bulle *et al.* 2010; this study). The original tectonic relationships are no longer preserved. As reported from other exhumed subduction-accretionary complexes around the world, superposition of different processes is very likely (e.g. Festa *et al.* 2019, 2022 and references therein). A ‘one-size-fits-all’ model is almost certainly wrong.

10. Concluding remarks

Jadeitites document processes that occur at or near the slab–mantle interface, followed by return flow in the subduction channel. Numerous studies have shown that jadeitites are mostly associated with exhumed serpentinite-matrix mélanges. However, in the CBU, jadeitites are occasionally (Syros) or exclusively (Tinos) found in clastic metasediments or meta-tuffaceous sequences. While an original relationship with ultramafic rocks is clearly documented for jadeitites from Syros by blackwalls or thin layers of serpentinitic schists around the blocks, such features are largely absent on Tinos. The most likely explanation for these observations is that the original field structures were reworked by various tectonic and sedimentary processes. The differences between the Kampos mélange on Syros and the block-in-matrix sequence on Tinos mainly concern the amount of serpentinite and the abundance of mélange blocks but do not indicate a significantly different origin.

This study further corroborates the importance of *c.* 80 Ma zircon ages for jadeitites from both islands, but their geological significance remains unclear. Interpretations suggesting that all jadeitites were formed by pervasive metasomatic replacement of a pre-existing rock are not fully supported by field observations, which indicate jadeitite precipitation in fractures in at least some cases. Both precipitation- and replacement-type processes may be documented by jadeitites and omphacitites of the study area.

A relationship between the jadeitite formation and the Eocene blueschist facies metamorphism recorded in associated rocks seems plausible at first, but this HP/LT event might have simply overprinted pre-existing jadeitite. So far, no exact age could be assigned to the formation of this rock type. More details are needed to understand the petrogenesis of the jadeitites from the CBU.

Supplementary material. The supplementary material for this article can be found at <https://doi.org/10.1017/S0016756823000602>

Availability of data and material. Full dataset available as Online Resource.

Code availability. Not applicable.

Acknowledgements. The author would like to thank M. Trogisch for thin section preparation and J. Berndt and B. Schmitte for help on the electron microprobe. A. Larionov, I. Paderin, S. Presnyakov and N. Rodionov are gratefully acknowledged for kind support and help with the SHRIMP analyses. The author would also like to thank Thomas Lamont and an anonymous reviewer for very helpful and constructive comments.

Financial support. This work was supported by a grant from the Deutsche Forschungsgemeinschaft BR 1068/13-1.

Competing interests. None.

References

- Ague JJ (2007) Models of permeability contrasts in subduction zone mélange: implications for gradients in fluid fluxes, Syros and Tinos Islands, Greece. *Chemical Geology* 239, 217–27. doi: [10.1016/j.chemgeo.2006.08.012](https://doi.org/10.1016/j.chemgeo.2006.08.012)
- Altherr R, Kreuzer H, Lenz H, Wendt I, Harre W and Dürr S (1994) Further evidence for Late-Cretaceous low pressure/high-temperature terrane in the Cyclades, Greece. *Chemie der Erde* 54, 319–28.
- Altherr R, Kreuzer H, Wendt I, Lenz H, Wagner GA, Keller J, Harre W and Höhndorf A (1982) A Late Oligocene/Early Miocene high temperature belt in the Attic-Cycladic Crystalline Complex (SE Pelagonian, Greece). *Geologisches Jahrbuch* E 23, 97–164.
- Altherr R, Schliestedt M, Okrusch M, Seidel E, Kreuzer H, Harre W, Lenz H, Wendt I and Wagner GA (1979) Geochronology of high-pressure rocks on

- Sifnos (Cyclades, Greece). *Contributions to Mineralogy and Petrology* **70**, 245–55. doi: [10.1007/bf00375354](https://doi.org/10.1007/bf00375354)
- Angiboust S, Glodny J, Cambeses A, Raimondo T, Monié P, Popov M and Garcia-Casco A** (2020) Drainage of subduction interface fluids into the forearc mantle evidenced by a pristine jadeitite network (Polar Urals). *Journal of Metamorphic Geology* **39**, 473–500. doi: [10.1111/jmg.12570](https://doi.org/10.1111/jmg.12570)
- Angiboust S, Muñoz-Montecinos J, Cambeses A, Raimondo T, Deldicque D and Garcia-Casco A** (2021) Jolts in the jade factory: a route for subduction fluids and their implications for mantle edge seismicity. *Earth-Science Reviews* **220**, 103720. doi: [10.1016/j.earscirev.2021.103720](https://doi.org/10.1016/j.earscirev.2021.103720)
- Avigad D and Garfunkel Z** (1989) Low angle shear zones underneath and above a Blueschist belt – Tinos Island, Cyclades, Greece. *Terra Nova* **1**, 182–87. doi: [10.1111/j.1365-3121.1989.tb00350.x](https://doi.org/10.1111/j.1365-3121.1989.tb00350.x)
- Be'eri-Shlevin Y, Avigad D and Matthews A** (2009) Granitoid intrusion and high temperature metamorphism in the Asteroussia Unit, Anafi Island (Greece): petrology and geochronology. *Israel Journal of Earth Sciences* **58**, 13–27. doi: [10.1560/ijes.58.1.13](https://doi.org/10.1560/ijes.58.1.13)
- Bolhar R, Ring U and Allen CM** (2010) An integrated zircon geochronological and geochemical investigation into the Miocene plutonic evolution of the Cyclades, Aegean Sea, Greece: Part 1: geochronology. *Contributions to Mineralogy and Petrology* **160**, 719–42. doi: [10.1007/s00410-010-0504-4](https://doi.org/10.1007/s00410-010-0504-4)
- Breeding CM, Ague JJ and Bröcker M** (2004) Fluid–metasedimentary rock interactions in subduction-zone mélange: implications for the chemical composition of arc magmas. *Geology* **32**, 1041–44. doi: [10.1130/g20877.1](https://doi.org/10.1130/g20877.1)
- Breeding CM, Ague JJ, Bröcker M and Bolton EW** (2003) Blueschist preservation in a retrograded, high-pressure, low-temperature metamorphic terrane, Tinos, Greece: implications for fluid flow paths in subduction zones. *Geochemistry, Geophysics, Geosystems* **4**. doi: [10.1029/2002GC000380](https://doi.org/10.1029/2002GC000380)
- Brichau S, Ring U, Carter A, Monié P, Bolhar R, Stockli D and Brunel M** (2007) Extensional faulting on Tinos Island, Aegean Sea, Greece: how many detachments? *Tectonics* **26**, TC4009. doi: [10.1029/2006TC001969](https://doi.org/10.1029/2006TC001969)
- Bröcker M, Baldwin S and Arkudas R** (2013) The geologic significance of $^{40}\text{Ar}/^{39}\text{Ar}$ and Rb–Sr white mica ages from Syros and Sifnos, Greece: a record of continuous (re)crystallization during exhumation? *Journal of Metamorphic Geology* **31**, 629–46. doi: [10.1111/jmg.12037](https://doi.org/10.1111/jmg.12037)
- Bröcker M, Bieling D, Hacker B and Gans P** (2004) High-Si phengite records the time of greenschist facies overprinting: Implications for models suggesting mega-detachments in the Aegean Sea. *Journal of Metamorphic Geology* **22**, 427–42. doi: [10.1111/j.1525-1314.2004.00524.x](https://doi.org/10.1111/j.1525-1314.2004.00524.x)
- Bröcker M and Enders M** (1999) U–Pb zircon geochronology of unusual eclogite-facies rocks from Syros and Tinos (Cyclades, Greece). *Geological Magazine* **136**, 111–8. doi: [10.1017/s0016756899002320](https://doi.org/10.1017/s0016756899002320)
- Bröcker M and Enders M** (2001) Unusual bulk-rock compositions in eclogite-facies rocks from Syros and Tinos (Cyclades, Greece): implications for U–Pb zircon geochronology. *Chemical Geology* **175**, 581–603. doi: [10.1016/S0009-2541\(00\)00369-7](https://doi.org/10.1016/S0009-2541(00)00369-7)
- Bröcker M and Franz L** (1994) The contact aureole on Tinos (Cyclades, Greece). Part I: field relationships, petrography and P–T conditions. *Chemie der Erde* **54**, 262–80.
- Bröcker M and Franz L** (1998) Rb–Sr isotope studies on Tinos Island (Cyclades, Greece): additional time constraints for metamorphism, extent of infiltration-controlled overprinting and deformational activity. *Geological Magazine* **135**, 369–82. doi: [10.1017/S0016756898008681](https://doi.org/10.1017/S0016756898008681)
- Bröcker M and Franz L** (2000) Contact metamorphism on Tinos (Cyclades, Greece): the importance of tourmaline, timing of the thermal overprint and Sr isotope characteristics. *Mineralogy and Petrology* **70**, 257–83. doi: [10.1007/s007100070006](https://doi.org/10.1007/s007100070006)
- Bröcker M and Franz L** (2005) The base of the Cycladic blueschist unit on Tinos Island (Greece) re-visited: Field relationships, phengite chemistry and Rb–Sr geochronology. *Neues Jahrbuch für Mineralogie Abhandlungen* **181**, 81–93. doi: [10.1127/0077-7757/2005/0181-0003](https://doi.org/10.1127/0077-7757/2005/0181-0003)
- Bröcker M and Keasling A** (2006) Ion probe U–Pb zircon ages from the high-pressure/low-temperature mélange of Syros, Greece: age diversity and the importance of pre-Eocene subduction. *Journal of Metamorphic Geology* **24**, 615–31. doi: [10.1111/j.1525-1314.2006.00658.x](https://doi.org/10.1111/j.1525-1314.2006.00658.x)
- Bröcker M, Kreuzer H, Matthews A and Okrusch M** (1993) $^{40}\text{Ar}/^{39}\text{Ar}$ and oxygen isotope studies of polymetamorphism from Tinos Island, Cycladic blueschist belt. *Journal of Metamorphic Geology* **11**, 223–40. doi: [10.1111/j.1525-1314.1993.tb00144.x](https://doi.org/10.1111/j.1525-1314.1993.tb00144.x)
- Bröcker M, Löwen K and Rodionov N** (2014) Unraveling protolith ages of meta-gabbros from Samos and the Attic–Cycladic Crystalline Belt, Greece: results of a U–Pb zircon and Sr–Nd whole rock study. *Lithos* **198–199**, 234–48. doi: [10.1016/j.lithos.2014.03.029](https://doi.org/10.1016/j.lithos.2014.03.029)
- Bulle F, Bröcker M, Gärtner C and Keasling A** (2010) Geochemistry and geochronology of HP mélanges from Tinos and Andros, Cycladic blueschist belt, Greece. *Lithos* **117**, 61–81. doi: [10.1016/j.lithos.2010.02.004](https://doi.org/10.1016/j.lithos.2010.02.004)
- Cárdenas-Párraga J, Garcia-Casco A, Blanco-Quintero IF, Rojas-Agramonte Y, Cambra KN and Harlow GE** (2021) A highly dynamic hot hydrothermal system in the subduction environment: geochemistry and geochronology of jadeitite and associated rocks of the Sierra Del Convento Mélange (eastern Cuba). *American Journal of Science* **321**, 822–87. doi: [10.2475/06.2021.06](https://doi.org/10.2475/06.2021.06)
- Cárdenas-Párraga J, García-Casco A, Harlow GE, Blanco-Quintero IF, Rojas-Agramonte Y and Kröner A** (2012) Hydrothermal origin and age of jadeitites from Sierra del Convento Mélange (Eastern Cuba). *European Journal of Mineralogy*, **24**, 313–31. doi: [10.1127/0935-1221/2012/0024-2171](https://doi.org/10.1127/0935-1221/2012/0024-2171)
- Cliff RA, Bond CE, Butler RWH and Dixon JE** (2017) Geochronological challenges posed by continuously developing tectonometamorphic systems, insights from Rb–Sr mica ages from the Cycladic Blueschist Belt, Syros (Greece). *Journal of Metamorphic Geology* **35**, 197–211. doi: [10.1111/jmg.12228](https://doi.org/10.1111/jmg.12228)
- Coleman RG** (1961) Jadeite deposits of the Clear Creek area, New Idria district, San Benito County, California. *Journal of Petrology* **2**, 209–47. doi: [10.1093/petrology/2.2.209](https://doi.org/10.1093/petrology/2.2.209)
- Compagnoni R, Rolfo F and Castelli D** (2012) Jadeitite from the Monviso meta-ophiolite, western Alps: occurrence and genesis. *European Journal of Mineralogy* **24**, 333–43. doi: [10.1127/0935-1221/2011/0023-2164](https://doi.org/10.1127/0935-1221/2011/0023-2164)
- Cooperdock EH, Raia NH, Barnes JD, Stockli DF and Schwarzenbach EM** (2018) Tectonic origin of serpentinites on Syros, Greece: geochemical signatures of abyssal origin preserved in a HP/LT subduction complex. *Lithos* **296**, 352–64. doi: [10.1016/j.lithos.2017.10.020](https://doi.org/10.1016/j.lithos.2017.10.020)
- Dixon JE and Ridley J** (1987) Syros. In *Chemical Transport in Metasomatic Processes* (ed HC Helgeson), pp. 489–501. Dordrecht: Reidel Publishing Company.
- Dürr S, Altherr R, Keller J, Okrusch M and Seidel E** (1978) The median Aegean crystalline belt: stratigraphy, structure, metamorphism, magmatism. In *Alps, Appennines, Hellenides* (eds H Closs, DH Roeder & K Schmidt), pp. 455–77. Stuttgart: Schweizerbart.
- Dürr S** (1986) Das Attisch-kykladische Kristallin. In *Geologie von Griechenland* (ed V. Jacobshagen), pp. 116–48. Berlin: Gebrüder Bornträger.
- Festa A, Barbero E, Remitti F, Ogata K and Pini GA** (2022) Mélanges and chaotic rock units: Implications for exhumed subduction complexes and orogenic belts. *Geosystems and Geoenvironment* **1**, 100030. doi: [10.1016/j.geo.2022.100030](https://doi.org/10.1016/j.geo.2022.100030)
- Festa A, Pini GA, Ogata K and Dilek Y** (2019) Diagnostic features and field-criteria in recognition of tectonic, sedimentary and diapiric mélanges in orogenic belts and exhumed subduction-accretion complexes. *Gondwana Research* **74**, 11–34. doi: [10.1016/j.gr.2019.01.003](https://doi.org/10.1016/j.gr.2019.01.003)
- Flansburg ME, Stockli DF, Poulaki EM and Soukis K** (2019) Tectonomagmatic and stratigraphic evolution of the Cycladic basement, Ios Island, Greece. *Tectonics* **38**, 2291–316. doi: [10.1029/2018TC005436](https://doi.org/10.1029/2018TC005436)
- Flores KE, Martens U, Harlow GE, Brueckner HK and Pearson N** (2013) Jadeitite formed during subduction: in situ zircon geochronology constraints from two different tectonic events in the Guatemala Suture Zone. *Earth and Planetary Science Letters* **371–372**, 67–81. doi: [10.1016/j.epsl.2013.04.015](https://doi.org/10.1016/j.epsl.2013.04.015)
- Forster MA and Lister GS** (2005) Several distinct tectono-metamorphic slices in the Cycladic eclogite–blueschist belt, Greece. *Contributions to Mineralogy and Petrology* **150**, 523–45. doi: [10.1007/s00410-005-0032-9](https://doi.org/10.1007/s00410-005-0032-9)
- Freund S, Haase KM, Keith M, Beier C and Garbe-Schönberg CD** (2014) Constraints on the formation of geochemically variable plagiogranite intrusions in the Troodos Ophiolite, Cyprus. *Contributions to Mineralogy and Petrology* **167**, 1–22. doi: [10.1007/s00410-014-0978-6](https://doi.org/10.1007/s00410-014-0978-6)
- Fu B, Paul B, Cliff J, Bröcker M and Bulle F** (2012) O–Hf isotope constraints on the origin of zircon in high-pressure mélange blocks and associated matrix rocks from Tinos and Syros, Greece. *European Journal of Mineralogy* **24**, 277–87. doi: [10.1127/0935-1221/2011/0023-2131](https://doi.org/10.1127/0935-1221/2011/0023-2131)

- Fu B, Valley JW, Kita NT, Spicuzza MJ, Paton C, Tsujimori T, Bröcker M and Harlow GE (2010) Multiple origins of zircons in jadeitite. *Contributions to Mineralogy and Petrology* **159**, 769–80. doi: [10.1007/s00410-009-0453-y](https://doi.org/10.1007/s00410-009-0453-y)
- García-Casco A, Rodríguez Vega A, Cárdenas Párraga J, Iturralde-Vinent MA, Lázaro C, Blanco Quintero I, Rojas-Agramonte Y, Kröner A, Núñez Cambra K, Millán G, Torres-Roldán RL and Carrasquilla S (2009) A new jadeitite jade locality (Sierra del Convento, Cuba): first report and some petrological and archaeological implications. *Contributions to Mineralogy and Petrology* **158**, 1–26. doi: [10.1007/s00410-008-0367-0](https://doi.org/10.1007/s00410-008-0367-0)
- Glodny J and Ring U (2022) The Cycladic Blueschist Unit of the Hellenic subduction orogen: Protracted high-pressure metamorphism, decompression and reimbrication of a diachronous nappe stack. *Earth Science Reviews* **224**, 103883. doi: [10.1016/j.earscirev.2021.103883](https://doi.org/10.1016/j.earscirev.2021.103883)
- Gorce JS, Caddick MJ, Baxter EF, Dragovic B, Schumacher JC, Bodnar RJ and Kendall JF (2021) Insight into the early exhumation of the cycladic blueschist unit, Syros, Greece: combined application of zoned garnet geochronology, thermodynamic modeling and quartz elastic barometry. *Geochemistry, Geophysics, Geosystems*, e2021GC009716. doi: [10.1029/2021gc009716](https://doi.org/10.1029/2021gc009716)
- Grasemann B, Huet B, Schneider DA, Rice AHN, Lemonnier N and Tschegg C (2018) Miocene postorogenic extension of the Eocene synorogenic imbricated Hellenic subduction channel: New constraints from Milos (Cyclades, Greece). *Geological Society of America Bulletin* **130**, 238–62. doi: [10.1130/b31731.1](https://doi.org/10.1130/b31731.1)
- Gyomlai T, Agard P, Marschall HR, Jolivet L and Gerdes A (2021) Metasomatism and deformation of block-in-matrix structures in Syros: the role of inheritance and fluid-rock interactions along the subduction interface. *Lithos* **386–387**, 105996. doi: [10.1016/j.lithos.2021.105996](https://doi.org/10.1016/j.lithos.2021.105996)
- Harlow GE and Sorensen SS (2005) Jade (nephrite and jadeitite) and serpentinite: metasomatic connections. *International Geology Review* **47**, 113–46. doi: [10.2747/0020-6814.47.2.113](https://doi.org/10.2747/0020-6814.47.2.113)
- Harlow GE, Tsujimori T and Sorensen SS (2015) Jadeitites and plate tectonics. *Annual Review of Earth and Planetary Sciences* **43**, 105–38. doi: [10.1146/annurev-earth-060614-105215](https://doi.org/10.1146/annurev-earth-060614-105215)
- Hertwig A, Maresch WV and Schertl H-P (2021) Jadeitite and related rocks in serpentinite mélanges from the Rio San Juan Complex, Dominican Republic: evidence for both isochemical replacement and metasomatic desilication of igneous protoliths with fluid-assisted jadeite growth. *Russian Geology and Geophysics* **62**, 496–524. doi: [10.2113/RGG20204265](https://doi.org/10.2113/RGG20204265)
- Hertwig A, McClelland WC, Kitajima K., Schertl H-P, Maresch WV, Stanek K, Valley JW and Sergeev SA (2016) Inherited igneous zircons in jadeitite predate high-pressure metamorphism and jadeitite formation in the Jagua Clara serpentinite mélange of the Rio San Juan Complex (Dominican Republic). *Contributions to Mineralogy and Petrology* **171**, 48. doi: [10.1007/s00410-016-1256-6](https://doi.org/10.1007/s00410-016-1256-6)
- Hinsken T, Bröcker M, Berndt J and Gärtner C (2016) Maximum sedimentation ages and provenance of metasedimentary rocks from Tinos Island, Cycladic blueschist belt, Greece. *International Journal of Earth Sciences* **105**, 1923–40. doi: [10.1007/s00531-015-1258-z](https://doi.org/10.1007/s00531-015-1258-z)
- Hinsken T, Bröcker M, Strauss H and Bulle F (2017) Geochemical, isotopic and geochronological characterization of listvenite from the Upper Unit on Tinos, Cyclades, Greece. *Lithos* **282–283**, 281–97. doi: [10.1016/j.lithos.2017.02.019](https://doi.org/10.1016/j.lithos.2017.02.019)
- Höhn M, Bröcker M and Berndt J (2022) The Jurassic meta-ophiolitic rocks of Cape Steno, Andros, Greece: a high-pressure/low-temperature mélange with Pelagonian affinity in the Cycladic Blueschist Unit? *International Journal of Earth Sciences* **111**, 949–68. doi: [10.1007/s00531-022-02161-w](https://doi.org/10.1007/s00531-022-02161-w)
- Janoušek V, Farrow CM and Erban V (2006) Interpretation of whole-rock geochemical data in igneous geochemistry: introducing Geochemical Data Toolkit (GCDkit). *Journal of Petrology* **47**, 1255–59. doi: [10.1093/petrology/egl013](https://doi.org/10.1093/petrology/egl013)
- Jolivet L and Brun JP (2010) Cenozoic geodynamic evolution of the Aegean. *International Journal of Earth Sciences* **99**, 109–38. doi: [10.1007/s00531-008-0366-4](https://doi.org/10.1007/s00531-008-0366-4)
- Jolivet L, Lecomte E, Huet B, Denèle Y, Lacombe O, Labrousse L, Le Pourhiet L and Mehl C (2010) The north cycladic detachment system. *Earth Planetary Science Letters* **289**, 87–104. doi: [10.1016/j.epsl.2009.10.032](https://doi.org/10.1016/j.epsl.2009.10.032)
- Katzir Y, Matthews A, Garfunkel Z and Schliestedt M (1996) The tectono-metamorphic evolution of a dismembered ophiolite (Tinos, Cyclades, Greece). *Geological Magazine* **133**, 237–54. doi: [10.1017/S0016756800008992](https://doi.org/10.1017/S0016756800008992)
- Keay S (1998) The Geological Evolution of the Cyclades, Greece: constraints from SHRIMP U–Pb Geochronology. PhD thesis, Australian National University, Canberra. Published thesis. doi: [10.25911/5d66671ad2b2f](https://doi.org/10.25911/5d66671ad2b2f)
- Keiter M, Ballhaus C and Tomaschek F (2011) A new geological map of the Island of Syros (Aegean Sea, Greece): implications for lithostratigraphy and structural history of the Cycladic Blueschist Unit. *Geological Society of America Special Paper* **481**. doi: [10.1130/2011.2481](https://doi.org/10.1130/2011.2481)
- Keiter M, Piepjohn K, Ballhaus C, Lagos M and Bode M (2004) Structural development of high-pressure metamorphic rocks on Syros island (Cyclades, Greece). *Journal of Structural Geology* **26**, 1433–45. doi: [10.1016/j.jsg.2003.11.027](https://doi.org/10.1016/j.jsg.2003.11.027)
- Kotowski AJ and Behr WM (2019) Length scales and types of heterogeneities along the deep subduction interface: Insights from exhumed rocks on Syros island, Greece. *Geosphere* **15**, 1038–65. doi: [10.1130/ges02037.1](https://doi.org/10.1130/ges02037.1)
- Kotowski AJ, Cisneros M, Behr WM, Stockli DF, Soukis K, Barnes JD and Ortega-Arroyo D (2022) Subduction, underplating, and return flow recorded in the Cycladic Blueschist Unit exposed on Syros, Greece. *Tectonics* **41**, e2020TC006528. doi: [10.1029/2020TC006528](https://doi.org/10.1029/2020TC006528)
- Kuhlemann J, Frisch W, Dunkl I, Kázmér M and Schmiedl G (2004) Miocene siliciclastic deposits of Naxos Island: geodynamic and environmental implications for the evolution of the Southern Aegean Sea (Greece). *Geological Society of America Special Paper* **378**, 51–65. doi: [10.1130/0-8137-2378-7.51](https://doi.org/10.1130/0-8137-2378-7.51)
- Lagos M, Scherer EE, Tomaschek F, Münker C, Keiter M, Berndt J and Ballhaus C (2007) High precision Lu–Hf geochronology of Eocene eclogite-facies rocks from Syros, Cyclades, Greece. *Chemical Geology* **243**, 16–35. doi: [10.1016/j.chemgeo.2007.04.008](https://doi.org/10.1016/j.chemgeo.2007.04.008)
- Lamont TN, Roberts NMW, Searle MP, Gopon P, Waters DJ and Millar I (2020a) The age, origin, and emplacement of the Tsiknias Ophiolite, Tinos, Greece. *Tectonics* **39**, e2019TC005677. doi: [10.1029/2019TC005677](https://doi.org/10.1029/2019TC005677)
- Lamont TN, Searle MP, Gopon P, Roberts NMW, Wade J, Palin RM and Waters DJ (2020b) The Cycladic Blueschist Unit on Tinos, Greece: cold NE subduction and SW directed extrusion of the Cycladic continental margin under the Tsiknias Ophiolite. *Tectonics* **39**, e2019TC005890. doi: [10.1029/2019TC005890](https://doi.org/10.1029/2019TC005890)
- Lamont TN, Searle MP, Waters DJ, Roberts NM, Palin RM, Smye A, Dyck B, Weller OM and St-Onge MR (2019) Compressional origin of the Naxos metamorphic core complex, Greece: structure, petrography, and thermobarometry. *Geological Society of America Bulletin* **132**, 149–97. doi: [10.1130/B31978.1](https://doi.org/10.1130/B31978.1)
- Laurent V, Huet B, Labrousse L, Jolivet L, Monie P and Augier R (2017) Extraneous argon in high-pressure metamorphic rocks: distribution, origin and transport in the Cycladic Blueschist Unit (Greece). *Lithos* **272**, 315–35. doi: [10.1016/j.lithos.2016.12.013](https://doi.org/10.1016/j.lithos.2016.12.013)
- Laurent V, Jolivet L, Roche V, Augier R, Scaillet S and Cardello GL (2016) Strain localization in a fossilized subduction channel: insights from the Cycladic Blueschist Unit (Syros, Greece). *Tectonophysics* **672**, 150–69. doi: [10.1016/j.tecto.2016.01.036](https://doi.org/10.1016/j.tecto.2016.01.036)
- Laurent V, Scaillet S, Jolivet L, Augier R and Roche V (2021) ⁴⁰Ar behaviour and exhumation dynamics in a subduction channel from multi-scale ⁴⁰Ar/³⁹Ar systematics in phengite. *Geochimica et Cosmochimica Acta* **311**, 141–173. doi: [10.1016/j.gca.2021.06.001](https://doi.org/10.1016/j.gca.2021.06.001)
- Löwen K, Bröcker M and Berndt J (2015) Depositional ages of clastic metasediments from Samos and Syros, Greece: results of a detrital zircon study. *International Journal of Earth Sciences* **104**, 205–20. doi: [10.1007/s00531-014-1058-x](https://doi.org/10.1007/s00531-014-1058-x)
- Ludwig KR (2012) *User's Manual for ISOPLOT version 3.75–4.15: Geochronological Toolkit for Microsoft Excel*. Berkeley: Berkeley Geochronology Center. Special Publication 5.
- Maluski H, Bonneau M and Kienast JR (1987) Dating the metamorphic events in the Cycladic area: ³⁹Ar/⁴⁰Ar data from metamorphic rocks of the island of Syros (Greece). *Bulletin de la Société Géologique de France* **3**, 833–42. doi: [10.2113/gssgfbull.iii.5.833](https://doi.org/10.2113/gssgfbull.iii.5.833)

- Marschall HR, Ludwig T, Altherr R, Kalt A and Tonarini S (2006) Syros metasomatic tourmaline: evidence for very high- $\delta^{11}\text{B}$ fluids in subduction zones. *Journal of Petrology* **47**, 1915–42. doi: [10.1093/ptrology/egl031](https://doi.org/10.1093/ptrology/egl031)
- Martha SO, Dörr W, Gerdes A, Petschick R, Schastok J, Xypolias P and Zulauf G (2016) New structural and U–Pb zircon data from Anafi crystalline basement (Cyclades, Greece): constraints on the evolution of a Late Cretaceous magmatic arc in the Internal Hellenides. *International Journal of Earth Sciences* **105**, 2031–60. doi: [10.1007/s00531-016-1346-8](https://doi.org/10.1007/s00531-016-1346-8)
- Mavrogenatos C, Magganis A, Kati M, Bröcker M and Voudouris, P (2021) Ophicalcites from the Upper Tectonic Unit on Tinos, Cyclades, Greece: mineralogical, geochemical and isotope evidence for their origin and evolution. *International Journal of Earth Sciences* **110**, 809–32. doi: [10.1007/s00531-021-01991-4](https://doi.org/10.1007/s00531-021-01991-4)
- McDonough WF and Sun S-S (1995) The composition of the Earth. *Chemical Geology* **120**, 223–53. doi: [10.1016/0009-2541\(94\)00140-4](https://doi.org/10.1016/0009-2541(94)00140-4)
- Melidonis NG (1980) The geological structure and mineral deposits of Tinos island (Cyclades, Greece). *The Geology of Greece* **13**, 1–80.
- Meng F, Yang H-J, Makeyev AB, Ren Y, Kulikova KV, Bryanchaninova NI (2016) Jadeite in the Syum-Keu ultramafic complex from Polar Urals, Russia: insights into fluid activity in subduction zones. *European Journal of Mineralogy* **28**, 1079–97. doi: [10.1127/ejm/2016/0028-2563](https://doi.org/10.1127/ejm/2016/0028-2563)
- Miller DP, Marschall HR, Schumacher JC (2009) Metasomatic formation and petrology of blueschist-facies hybrid rocks from Syros (Greece): implications for reactions at the slab-mantle interface. *Lithos* **107**, 53–67. doi: [10.1016/j.lithos.2008.07.015](https://doi.org/10.1016/j.lithos.2008.07.015)
- Mori Y, Orihashi Y, Miyamoto T, Shimada K, Shigeno M, Nishiyama T (2011) Origin of zircon in jadeite from the Nishisonogi metamorphic rocks, Kyushu Japan. *Journal of Metamorphic Geology* **29**, 673–84. doi: [10.1111/j.1525-1314.2011.00935.x](https://doi.org/10.1111/j.1525-1314.2011.00935.x)
- Morimoto N, Fabries J, Ferguson AK, Ginzburg IV, Ross M, Seifert FA, Zussman J, Aoki K and Gottardi G (1988) Nomenclature of pyroxenes. *Mineralogy and Petrology* **39**, 55–76.
- Okrusch M and Bröcker M (1990) Eclogite facies rocks in the Cycladic blueschist belt, Greece: a review. *European Journal of Mineralogy* **2**, 451–78. doi: [10.1127/ejm/2/4/0451](https://doi.org/10.1127/ejm/2/4/0451)
- Parra T, Vidal O and Jolivet L (2002) Relation between the intensity of deformation and retrogression in blueschist metapelites of Tinos Island (Greece) evidenced by chlorite-mica local equilibria. *Lithos* **63**, 41–66. doi: [10.1016/s0024-4937\(02\)00115-9](https://doi.org/10.1016/s0024-4937(02)00115-9)
- Patzak M, Okrusch M and Kreuzer H (1994) The Akrotiri unit on the island of Tinos, Cyclades, Greece: witness to a lost terrane of Late Cretaceous age. *Neues Jahrbuch für Geologie und Paläontologie Abhandlungen* **194**, 211–52. doi: [10.1127/njgpa/194/1994/211](https://doi.org/10.1127/njgpa/194/1994/211)
- Peilod A, Ring U, Glodny J and Skelton A (2017) An Eocene/Oligocene blueschist/greenschist-facies *P-T* loop from the Cycladic Blueschist Unit on Naxos Island, Greece: deformation-related reequilibration vs thermal relaxation. *Journal of Metamorphic Geology* **35**, 805–30. doi: [10.1111/jmg.12256](https://doi.org/10.1111/jmg.12256)
- Perraki M and Mposkos E (2001) New constraints for the alpine HP metamorphism of the Ios basement, Cyclades, Greece. *Bulletin of the Geological Society of Greece* **34**, 977–84. doi: [10.12681/bgsg.17130](https://doi.org/10.12681/bgsg.17130)
- Philippon M, Brun JP and Gueydan F (2011) Tectonics of the Syros blueschists (Cyclades, Greece): From subduction to Aegean extension. *Tectonics* **30**, TC4001. doi: [10.1029/2010TC002810](https://doi.org/10.1029/2010TC002810)
- Poulaki EM, Stockli DF, Flansburg ME and Soukis K (2019) Zircon U–Pb chronostratigraphy and provenance of the Cycladic Blueschist Unit and Cycladic Basement on Sikinos and Ios Islands, Greece. *Tectonics*. doi: [10.1029/2018TC005436](https://doi.org/10.1029/2018TC005436)
- Putlitz B, Cosca MA and Schumacher JC (2005) Prograde mica $^{40}\text{Ar}/^{39}\text{Ar}$ growth ages recorded in high pressure rocks (Syros, Cyclades, Greece). *Chemical Geology* **214**, 79–98. doi: [10.1016/j.chemgeo.2004.08.056](https://doi.org/10.1016/j.chemgeo.2004.08.056)
- Ridley JR (1984) Listric normal faulting and the reconstruction of the synmetamorphic structural pile of the Cyclades. In *The Geological Evolution of the Eastern Mediterranean* (eds JE Dixon & AHF Robertson), pp. 755–61: Geological Society of London, Special Publication no. 17. doi: [10.1144/GSL.SP.1984.017.01.60](https://doi.org/10.1144/GSL.SP.1984.017.01.60)
- Ring U, Glodny J, Will J and Thomson SN (2010) The Hellenic subduction system: high-pressure metamorphism, exhumation, normal faulting, and large-scale extension. *Annual Review of Earth and Planetary Sciences* **38**, 45–76. doi: [10.1146/annurev.earth.050708.170910](https://doi.org/10.1146/annurev.earth.050708.170910)
- Ring U, Laws S and Bernet M (1999) Structural analysis of a complex nappe sequence and late-orogenic basins from the Aegean Island of Samos, Greece. *Journal of Structural Geology* **21**, 1575–601. doi: [10.1016/s0191-8141\(99\)00108-x](https://doi.org/10.1016/s0191-8141(99)00108-x)
- Ring U, Pantazides H, Glodny J and Skelton A (2020) Forced return flow deep in the subduction channel, Syros, Greece. *Tectonics* **39**, e2019TC005768. doi: [10.1029/2019TC005768](https://doi.org/10.1029/2019TC005768)
- Ring U, Thomson SN and Bröcker M (2003) Fast extension but little exhumation: the Vari detachment in the Cyclades, Greece. *Geological Magazine* **140**, 245–52. doi: [10.1017/S0016756803007799](https://doi.org/10.1017/S0016756803007799)
- Rogowitz A, Huet B, Schneider D and Grasmann B (2015). Influence of high strain rate deformation on $^{40}\text{Ar}/^{39}\text{Ar}$ mica ages from marble mylonites (Syros, Greece). *Lithosphere* **7**, 535–40. doi: [10.1130/L455.1](https://doi.org/10.1130/L455.1)
- Rollinson HR (2009) New models for the genesis of plagiogranites in the Oman ophiolite. *Lithos* **112**, 603–14. doi: [10.1016/j.lithos.2009.06.006](https://doi.org/10.1016/j.lithos.2009.06.006)
- Sanchez-Gomez M, Avigad D and Heimann A (2002) Geochronology of clasts in allochthonous Miocene sedimentary sequences on Mykonos and Paros islands: implications for back-arc extension in the Aegean Sea. *Journal of the Geological Society* **159**, 45–60. doi: [10.1144/0016-764901031](https://doi.org/10.1144/0016-764901031)
- Schaltegger U (2007) Hydrothermal zircon. *Elements* **3**, 51. doi: [10.2113/gselements.3.1.51](https://doi.org/10.2113/gselements.3.1.51)
- Schertl HP, Maresch WV, Stanek KP, Hertwig A, Krebs M, Baese R and Sergeev SS (2012) New occurrences of jadeite, jadeite quartzite and jadeite-lawsonite quartzite in the Dominican Republic, Hispaniola: petrological and geochronological overview. *European Journal of Mineralogy* **24**, 199–216.
- Schumacher JC, Brady JB, Cheney JT and Tonnsen RR (2008) Glaucophane-bearing marbles on Syros, Greece. *Journal of Petrology* **49**, 1667–86. doi: [10.1093/ptrology/egn042](https://doi.org/10.1093/ptrology/egn042)
- Seck HA, Koetz J, Okrusch M, Seidel E and Stosch H-G (1996) Geochemistry of a meta-ophiolite suite: an association of metagabbros, eclogites and glaucophanites on the island of Syros, Greece. *European Journal of Mineralogy* **8**, 607–24. doi: [10.1127/ejm/8/3/0607](https://doi.org/10.1127/ejm/8/3/0607)
- Seman S (2016) The tectonostratigraphy of the Cycladic Blueschist Unit and new garnet geo/thermochronology techniques. PhD thesis, The University of Texas, Austin. Published thesis. doi: [10.15781/T20K26H0W](https://doi.org/10.15781/T20K26H0W)
- Seman S, Stockli D and Soukis K (2017) The provenance and internal structure of the Cycladic Blueschist Unit revealed by detrital zircon geochronology, Western Cyclades, Greece. *Tectonics* **36**, 1407–29. doi: [10.1002/2016tc004378](https://doi.org/10.1002/2016tc004378)
- Shaked Y, Avigad D and Garfunkel Z (2000) Alpine high-pressure metamorphism of the Almyropotamos window (southern Evia, Greece). *Geological Magazine* **137**, 367–80. doi: [10.1017/s001675680000426x](https://doi.org/10.1017/s001675680000426x)
- Sheng YM, Zheng YF, Chen RX, Li QL and Dai MN (2012) Fluid action on zircon growth and recrystallization during quartz veining within UHP eclogite: insights from U–Pb ages, O–Hf isotopes and trace elements. *Lithos* **136–139**, 126–44. doi: [10.1016/j.lithos.2011.06.012](https://doi.org/10.1016/j.lithos.2011.06.012)
- Shigeno M, Mori Y, Shimada K and Nishiyama T (2012) Origin of omphacitites from the Nishisonogi metamorphic rocks, western Kyushu, Japan: comparison with jadeitites. *European Journal of Mineralogy* **24**, 247–62. doi: [10.1127/0935-1221/2012/0024-2198](https://doi.org/10.1127/0935-1221/2012/0024-2198)
- Skelton A, Peilod A, Glodny J, Klonowska I, Manbro C, Lodin K and Ring U (2019) Preservation of high-P rocks coupled to rock composition and the absence of metamorphic fluids. *Journal of Metamorphic Geology* **37**, 359–81. doi: [10.1111/jmg.12466](https://doi.org/10.1111/jmg.12466)
- Soukis K and Stockli DF (2013) Structural and thermochronometric evidence for multi-stage exhumation of southern Syros, Cycladic Islands, Greece. *Tectonophysics* **595–596**, 148–64. doi: [10.1016/j.tecto.2012.05.017](https://doi.org/10.1016/j.tecto.2012.05.017)
- Stacey JS and Kramers JD (1975) Approximation of terrestrial lead isotope evolution by a two-stage model. *Earth and Planetary Science Letters* **26**, 207–21.
- Stolz J, Engi M and Rickli M (1997) Tectonometamorphic evolution of SE Tinos, Cyclades. *Schweizerische Mineralogische und Petrographische Mitteilungen* **77**, 209–31. doi: [10.5169/seals-58481](https://doi.org/10.5169/seals-58481)
- Sun SS and McDonough WF (1989) Chemical and isotopic systematics of oceanic basalts: implications for mantle composition and processes. In *Magmatism in the Ocean Basins* (eds AD Saunders & MJ Norry), pp. 313–45:

- Geological Society of London, Special Publication no 42. doi: [10.1144/GSL.SP.1989.042.01.19](https://doi.org/10.1144/GSL.SP.1989.042.01.19)
- Tomaschek F, Baumann A, Villa IM, Kennedy A and Ballhaus C** (2000) Geochronological constraints on a Cretaceous metamorphic event from the Vari Unit (Syros, Cyclades, Greece). *Beihefte zum European Journal of Mineralogy* **12**, 214.
- Tomaschek F, Keiter M, Kennedy AK and Ballhaus C** (2008) Pre-Alpine basement within the Northern Cycladic Blueschist Unit on Syros Island, Greece. *Zeitschrift der Deutschen Gesellschaft für Geowissenschaften* **159**, 521–31. doi: [10.1127/1860-1804/2008/0159-0521](https://doi.org/10.1127/1860-1804/2008/0159-0521)
- Tomaschek F, Kennedy AK, Villa IM, Lagos M, Ballhaus C** (2003) Zircons from Syros, Cyclades, Greece. Recrystallization and mobilization of zircon during high-pressure metamorphism. *Journal of Petrology* **44**, 1977–2002. doi: [10.1093/ptrology/egg067](https://doi.org/10.1093/ptrology/egg067)
- Trotet F, Jolivet L and Vidal O** (2001a) Tectono-metamorphic evolution of Syros and Sifnos islands (Cyclades, Greece). *Tectonophysics* **338**, 179–206. doi: [10.1016/S0040-1951\(01\)00138-X](https://doi.org/10.1016/S0040-1951(01)00138-X)
- Trotet F, Vidal O and Jolivet L** (2001b) Exhumation of Syros and Sifnos metamorphic rocks (Cyclades, Greece). New constraints on the PT paths. *European Journal of Mineralogy* **13**, 901–20. doi: [10.1127/0935-1221/2001/0013/0901](https://doi.org/10.1127/0935-1221/2001/0013/0901)
- Tsujimori T and Harlow GE** (2012) Petrogenetic relationships between jadeitite and associated high-pressure and low-temperature metamorphic rocks in worldwide jadeitite localities: a review. *European Journal of Mineralogy* **24**, 371–90. doi: [10.1127/0935-1221/2012/0024-2193](https://doi.org/10.1127/0935-1221/2012/0024-2193)
- Tual L, Smit MA, Cutts J, Kooijman E, Kielman-Schmitt M, Majka J and Foulds I** (2022) Rapid, paced metamorphism of blueschists (Syros, Greece) from laser-based zoned Lu-Hf garnet chronology and LA-ICPMS trace element mapping. *Chemical Geology* **607**, 121003. doi: [10.1016/j.chemgeo.2022.121003](https://doi.org/10.1016/j.chemgeo.2022.121003)
- Uunk B, Brouwer F, de Paz-Álvarez M, van Zuilen K, Huybens R, van 't Veer R and Wijbrans J** (2022) Consistent detachment of supracrustal rocks from a fixed subduction depth in the Cyclades. *Earth and Planetary Science Letters* **584**. doi: [10.1016/j.epsl.2022.117479](https://doi.org/10.1016/j.epsl.2022.117479)
- Uunk B, Brouwer F, ter Voorde M and Wijbrans J** (2018) Understanding phengite ar-gon closure using single grain fusion age distributions in the Cycladic Blueschist Unit on Syros, Greece. *Earth and Planetary Science Letters* **484**, 192–203. doi: [10.1016/j.epsl.2017.12.031](https://doi.org/10.1016/j.epsl.2017.12.031)
- Van der Maar PA** (1980) The geology and petrology of Ios, Cyclades, Greece. *Annales Géologiques des Pays Helléniques* **30**, 206–24.
- Van der Maar PA, Jansen JBH** (1983) The geology of the polymetamorphic complex of Ios, Cyclades, Greece and its significance for the Cycladic Massif. *Geologische Rundschau* **72**, 283–99. doi: [10.1007/bf01765910](https://doi.org/10.1007/bf01765910)
- Wijbrans JR, Schliestedt M and York D** (1990) Single grain argon laser probe dating of phengites from the blueschist to greenschist transition on Sifnos (Cyclades, Greece). *Contributions to Mineralogy and Petrology* **104**, 582–93. doi: [10.1007/bf00306666](https://doi.org/10.1007/bf00306666)
- Wolfe OM, Spear FS, Thomas JB, Hasegawa EM, Libby GT and Cheney JT** (2023) Pressure-temperature evolution of the basement and cover sequences on Ios, Greece: evidence for subduction of the Hercynian basement. *Journal of Metamorphic Geology*, 1–23. doi: [10.1111/jmg.12738](https://doi.org/10.1111/jmg.12738)
- Yui T-F and Fukuyama M** (2015) A revisit to the Yorii jadeite-quartz rock, the Kanto Mountains, central Japan: Implications for petrogenesis. *Journal of Asian Earth Sciences* **108**, 58–67. doi: [10.1016/j.jseas.2015.04.022](https://doi.org/10.1016/j.jseas.2015.04.022)
- Yui TF, Maki K, Usuki T, Lan CY, Martens U, Wu CM, Wu TW and Liou JG** (2010) Genesis of Guatemala jadeitite and related fluid characteristics: insight from zircon. *Chemical Geology* **270**, 45–55. doi: [10.1016/j.chemgeo.2009.11.004](https://doi.org/10.1016/j.chemgeo.2009.11.004)
- Zeffren S, Avigad D, Heimann A and Gvirtzman Z** (2005) Age resetting of hanging wall rocks above a low-angle detachment shear zone: Tinos Island (Aegean Sea). *Tectonophysics* **400**, 1–25. doi: [10.1016/j.tecto.2005.01.003](https://doi.org/10.1016/j.tecto.2005.01.003)
- Zhong S, Feng C, Seltmann R, Li D and Qu, H** (2018) Can magmatic zircon be distinguished from hydrothermal zircon by trace element composition? The effect of mineral inclusions on zircon trace element composition. *Lithos* **314–315**, 646–57. doi: [10.1016/j.lithos.2018.06.029](https://doi.org/10.1016/j.lithos.2018.06.029)